Effects of slight nose bluntness and roughness on boundary-layer transition in supersonic flows

By J. LEITH POTTER AND JACK D. WHITFIELD

ARO, Inc., Tullahoma, Tennessee

(Received 27 April 1961 and in revised form 13 November 1961)

1. Introduction

It is the purpose of this paper to report an investigation concerning certain factors affecting transition from laminar to turbulent flow in boundary layers. The objectives of the investigation were to clarify further the effects of very small degrees of leading-edge bluntness, and to devise a means for estimating the effect of roughness on boundary-layer transition.

The unit Reynolds number, or Reynolds number per unit length, is given particular attention in the analysis of the data presented here because of plentiful evidence that the commonly used forms of Reynolds number describing transition generally vary with the unit Reynolds number. This occurs in subsonic and supersonic wind tunnels, and there are data from free-flight tests showing the same behaviour. It is obvious that at least a part of this is due to the relation between unit Reynolds number and roughness, leading-edge bluntness, and wind-tunnel turbulence and noise. However, there could be more significance to this factor (Whitfield & Potter 1958) and it deserves consideration in any case.

Even small degrees of nose bluntness having negligible effect on measured pressure distributions have a noticeable effect on boundary-layer transition. Therefore, if one is to compare data from different models or estimate the effect of bluntness alone in influencing transition, some general quantitative evaluation is needed.

The requirement for a reliable method for estimating the effect of both two- and three-dimensional roughness at supersonic speeds is recognized. The difficulty in simulating naturally turbulent boundary layers on small models in hypersonic flow is acute. It is probably true that fully developed turbulent boundary layers never have been attained on models in many existing hypersonic and hypervelocity test facilities. Of course, this is partly due to the fact that high Mach and Reynolds numbers seldom are attained simultaneously in a wind tunnel.

Each of these problems will be discussed in the following sections; the conclusions are given as a final summary.

2. Symbols

a	speed of sound
b	leading edge thickness (see figures 1 and 2)
$\overline{e^2}$	mean-square hot-wire output, arbitrary units
k	height of roughness element
M	Mach number
p	pressure
p_0'	pitot pressure
Re	Reynolds number
Re_b	$(U/\nu)_\infty b$
Re_k	$u_k k/\nu_k$
Re_k^*	$a^* k/\nu^*$
Re_k'	$Re_k(M_p/M_k)\,(p_p/p_\delta)\,(T_k/T_w)^{0\cdot5+\omega}$
Re_t	Reynolds number of transition, $U_\delta x_t/\nu_\delta$
$(Re_t)_{end}$	Reynolds number at onset of fully developed turbulent flow (see figure 3)
Re_{to}	Reynolds number of transition on a body with no surface roughness
Re_{x_k}	$U_\delta x_k/\nu_\delta$
$Re_{\Delta x}$	$U_\delta \Delta x/\nu_\delta$
T	temperature
U	velocity in free stream or at outer edge of boundary layer
u	velocity in the boundary layer
x	wetted distance along surface measured from stagnation point
Δx	longitudinal extent of transition region
y	vertical distance above surface measured from surface
γ	ratio of specific heats of air
δ	total boundary-layer thickness
δ^*	boundary-layer displacement thickness
η_r	temperature recovery factor, $(T_w - T_\delta)/(T_0 - T_\delta)$
ϵ	value of Re_k', where $x_t = x_k$
θ	bevel angle of lower leading edge (see figures 1 and 2)
μ	dynamic viscosity
ν	kinematic viscosity, μ/ρ
ρ	mass density
ω	exponent in viscosity-temperature relation

Subscripts:

b	leading edge thickness (see figures 1 and 2)
c	critical
k	at height k in undisturbed, laminar boundary layer at station x_k (except δ_k)
0	stagnation conditions
p	plateau value in region of roughness element
t	at transition
to	at transition on smooth body ($k = 0$)

w	body surface conditions
aw	surface conditions for adiabatic recovery temperature
δ	edge of boundary layer
∞	free stream

Superscripts:

*	sonic condition (except δ^*)

3. Experimental apparatus and techniques

Wind tunnels

The 12×12 in. supersonic wind tunnel (Anderson 1958) and the 50 in. diam. hypersonic wind tunnel (Sivells 1959) of the von Karman Gas Dynamics Facility (VKF) were utilized for the experimental phase of this study.

Models

The basic models were hollow cylinders, with measurements being accomplished on the exterior surface. Two sizes were required, a 3 in. diam. cylinder was used in the 12 in. tunnel and a 6 in. diam. cylinder was used in the 50 in. diam. tunnel. The interior surface finish of all models was about 20 μin. rms.

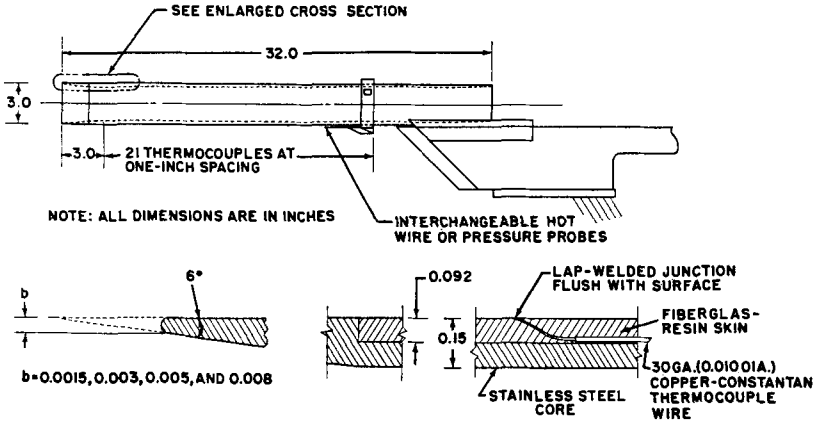

FIGURE 1. 3 in. diam. hollow-cylinder model.

(1) *3 in. diam. hollow cylinder* (figure 1). This cylinder was constructed of laminated Fiberglas and epoxy resin over a stainless-steel tubular core. Twenty-one surface thermocouples and three static-pressure tubes were imbedded in the Fiberglas-resin skin. A surface finish of 10 to 15 μin. rms was obtained on the epoxy-resin surface. Four interchangeable noses with an internal angle of 6 deg. and with leading-edge thicknesses of 0·0015, 0·003, 0·005 and 0·008 in. were tested.

(2) *6 in. diam. hollow cylinders* (figure 2). Two models, an instrumented cylinder and a non-instrumented cylinder, were constructed for the hypersonic experiments. The non-instrumented model was constructed of stainless steel and had a surface finish of 10 μin. rms. The instrumented model was constructed with 41 surface thermocouples and 12 static-pressure tubes imbedded in hot-sprayed aluminum oxide. The relative porosity of the aluminum oxide makes an accurate

estimate of the surface finish difficult. Conventional machine-shop practice will produce readings of 100 to 200 μin. rms. However, comparisons of transition locations on the two cylinders agree, indicating the instrumented cylinder to be aerodynamically smooth at a Mach number of 8. This model was tested with a leading edge thickness of 0·002 in. and with an internal bevel angle of 11·5 deg.

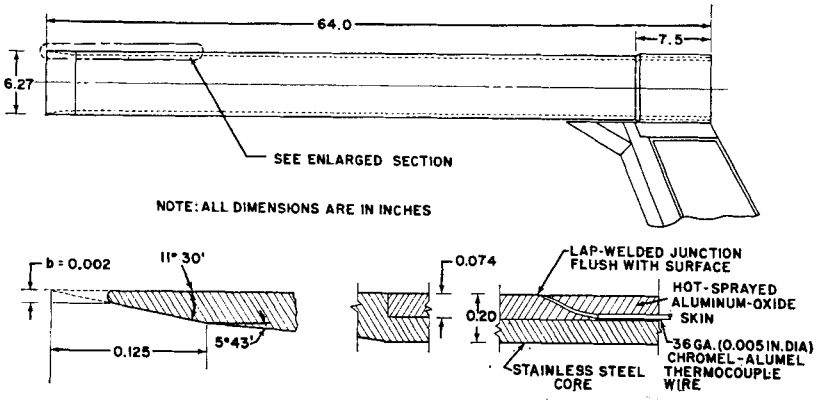

FIGURE 2. 6 in. diam. hollow-cylinder model.

Instrumentation

The hot-wire equipment was developed by Kovasznay (1954) at Johns Hopkins University. Minor modifications have been made in attempts to improve the signal-to-noise ratio and to permit the automatic recording of data.

Hot-wire surveys of the boundary layer from the laminar region to fully developed turbulent flow were made at selected test conditions. The hot-wire is, of course, sensitive to a combination of variables (velocity, density, and temperature) and the relative sensitivity to fluctuations of these quantities changes as the mean flow changes.

The simplest types of surveys were accomplished by maintaining the hot-wire at a constant current and traversing the wire longitudinally at constant vertical distance above the model surface. This was repeated at various heights. These are referred to as the 'constant current' traces and were used to construct the isolines of constant hot-wire output presented here.

The second, and more time-consuming, method consisted of positioning the wire at a given x-position and taking data from the hot-wire for several wire currents at each y-position. The sensitivity variations of the wire could then be approximated and the data corrected accordingly. This latter method, referred to as constant temperature, was used only within laminar-flow regions. The qualitative distribution of fluctuations within the laminar boundary layer is comparable for the two techniques at moderate wire temperatures, approximately 250 °F (see figure 15). It was found in certain low-density flow conditions that the constant current operation produced an excessive wire temperature as the hot-wire traversed the lower portion of the boundary layer. This caused large changes in sensitivity. The constant temperature method was used under such low-density conditions.

The hot-wires used in this study were 0·00015 in. diam. and 0·0003 in. diam. by 0·10 in. long tungsten wires for operation up to Mach number 5. The Mach number 8 testing was accomplished with platinum-coated tungsten wires of 0·0003 in. diam. and 0·10 in. length. Successful operation with the latter wires in the higher temperature Mach 8 flow was accomplished at moderate wire temperatures ($\approx$ 1000 °F). The general use of these wires in high-temperature flow is not recommended since an irreversible resistance rise occurred above 1000 °F. Other wire materials are being studied currently to find a wire suitable for higher temperatures.

Surface temperatures, schlieren photographs, and the boundary-layer pressure profiles were obtained with conventional wind-tunnel instrumentation. The impact-pressure variation along the surface was obtained from a 0·02 in. high by 0·04 in. wide, elliptically shaped pitot tube mounted against the surface in such a manner as to allow it to slide on the model surface. This tube was connected to a pressure transducer mounted directly to the probe holder to decrease response time.

4. The transition process

Definition of the transition region

It is well known that transition of the boundary layer from laminar to fully developed turbulent flow occurs over a distance of many boundary-layer thicknesses. In a strict sense then the concept of a transition point is ambiguous. However, it is common practice to adopt some definition of the transition point for purposes of analysis, and it has been shown that the influence of transition on certain transition-sensitive quantities can be accurately evaluated using an effective location which approximates the middle of the transition zone. Experimental studies of various factors influencing the transition process may be accomplished with an arbitrary, but consistent, definition of transition location provided that similarity of the mean transition process is retained.

The *beginning of transition* was taken as the point of initial measurable deviation of the boundary-layer thickness from a laminar rate of growth. Such a point is not well defined since it is located by seeking small deviations from an already somewhat arbitrarily defined quantity, boundary-layer thickness, δ. Fortunately, it will be seen that this is not a critical point. The *end of transition* was defined as the point where a fully developed turbulent growth was indicated.

Methods of transition detection

The five methods used to detect transition were: (1) change in rate of boundary-layer growth, (2) average visual indication from schlieren photographs, (3) maximum surface temperature location, (4) location of maximum output from a hot-wire traversed near the surface, and (5) location of maximum pressure from a pitot tube tranversed along the model surface.

Boundary-layer growth was obtained from the mean hot-wire resistance variations and from boundary-layer pressure profiles. The hot-wire technique consisted of observing the increase in mean hot-wire resistance as the hot-wire entered the boundary layer and thus locating the edge of the boundary layer.

The average schlieren indications of transition were obtained from a numerical average of locations read from a large number (10 to 40) of schlieren photographs taken at each test condition. A typical result of these photographs is shown in figure 3. This analysis is based on 36 spark schlieren photographs. It is apparent that a large deviation from the average indication may exist in a given photograph. It should be noted that these photographs were taken with a conventional

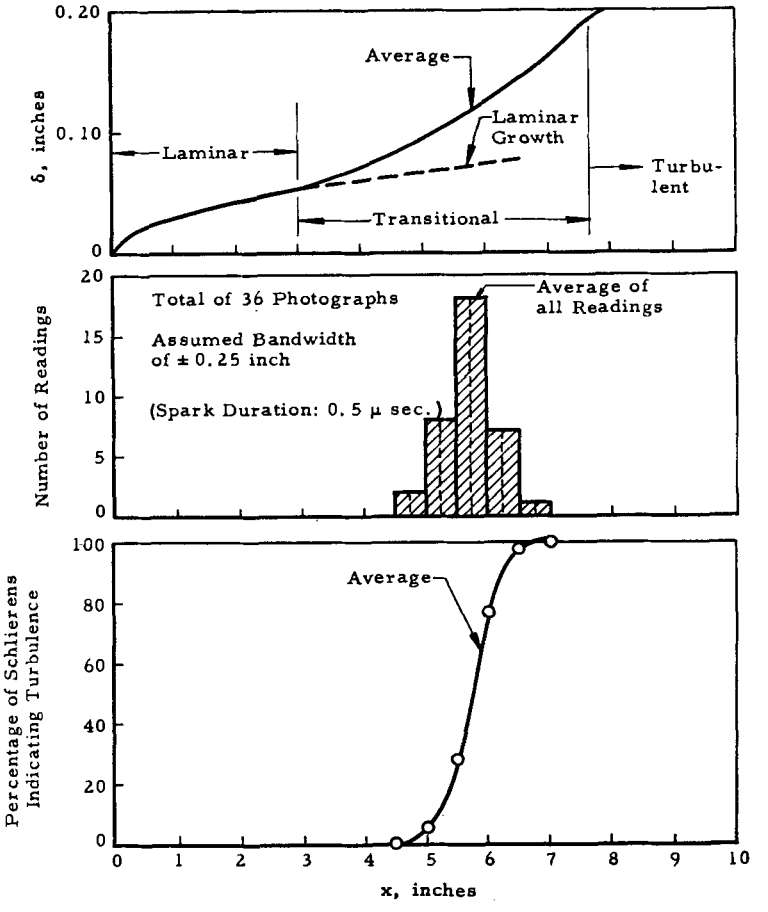

FIGURE 3. Analysis of spark schlieren photographs. $M_\infty = 4{\cdot}5$, $b = 0{\cdot}003$ in., $U_\infty/\nu_\infty = 350{,}000$/in.

wind-tunnel schlieren system using a spark of short duration, approximately $0{\cdot}5\ \mu$sec. The data-spread obtained from these photographs is due, in a large part, to the uncertainty in reading the photographs and should not be interpreted as a measure of the oscillation of the transition region.

Relatively early in our use of the hot-wire anemometer to detect transition, it became apparent that the transition region was not characterized by a sudden and violent onset of fluctuations but was rather an orderly, developing process which appeared to originate at or near the leading edge. The hot-wire was used to survey the entire boundary-layer flow field. Most of these surveys were taken with a wire operated at a constant current. These data are presented here in terms of

isoline diagrams of constant hot-wire output, $\overline{e^2}$, which is the mean-square signal from the hot-wire equipment. Such a diagram for $M_\infty = 3{\cdot}5$ is shown in figure 4. An electronic squaring circuit developed by Kovasznay (1954) was used to obtain this mean signal. The 'noise' noted here and in later figures refers to the electronic noise of the hot-wire equipment. The locations shown for the 'noise' level correspond to the condition where the hot-wire signal and electronic noise are approximately equal. These diagrams are interesting because of the pictorial

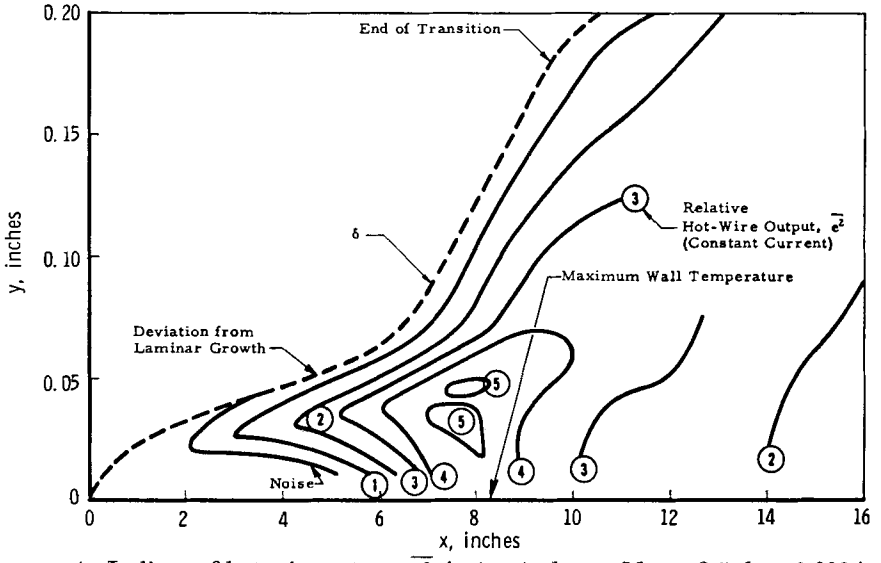

FIGURE 4. Isolines of hot-wire output, $\overline{e^2}$, in (x, y)-plane. $M_\infty = 3{\cdot}5$, $b = 0{\cdot}008$ in., $U_\infty/\nu_\infty = 270{,}000$/in.

representations of the transition process. A salient feature is the relatively intense stratification of fluctuations observed in the laminar region and the early portion of the transition region. This 'critical layer', which is indicated by stability theory (Rayleigh 1880 or Schlichting 1955), has been found in incompressible flow by Schubauer & Skramstad (1948) and has been observed in supersonic flow by Laufer & Vrebalovich (1958) and Demetriades (1958). However, these earlier experiments were concerned with studies of laminar instability, so none of these data enabled comparison of the magnitude of fluctuations in the laminar region and those in the transition region. The fact that these disturbances are of the same order creates a source of error in the determination of a transition 'point' from hot-wire traverses at heights above the surface, since a different point might be indicated for each different height of the probe above the surface.

In figure 4 one sees that a maximum hot-wire output for $y \to 0$ can be located with reasonable precision. The measurement of surface temperature distributions on the same model revealed that this maximum hot-wire signal near the surface corresponded to the maximum surface temperature, as noted in figure 4. Comparisons of the various methods of detection are shown in figure 5 for $M_\infty = 3{\cdot}5$. It may be observed that the similarity between the maximum hot-wire signal and the maximum surface temperature extends into the fully developed turbulent region where the hot-wire signal and the surface temperature become

substantially constant. Similar measurements for $M_\infty = 5$ are shown in figure 6. The same relative relation exists between all the various methods of transition detection. Behaviour of the different methods of transition detection is shown in figure 7.

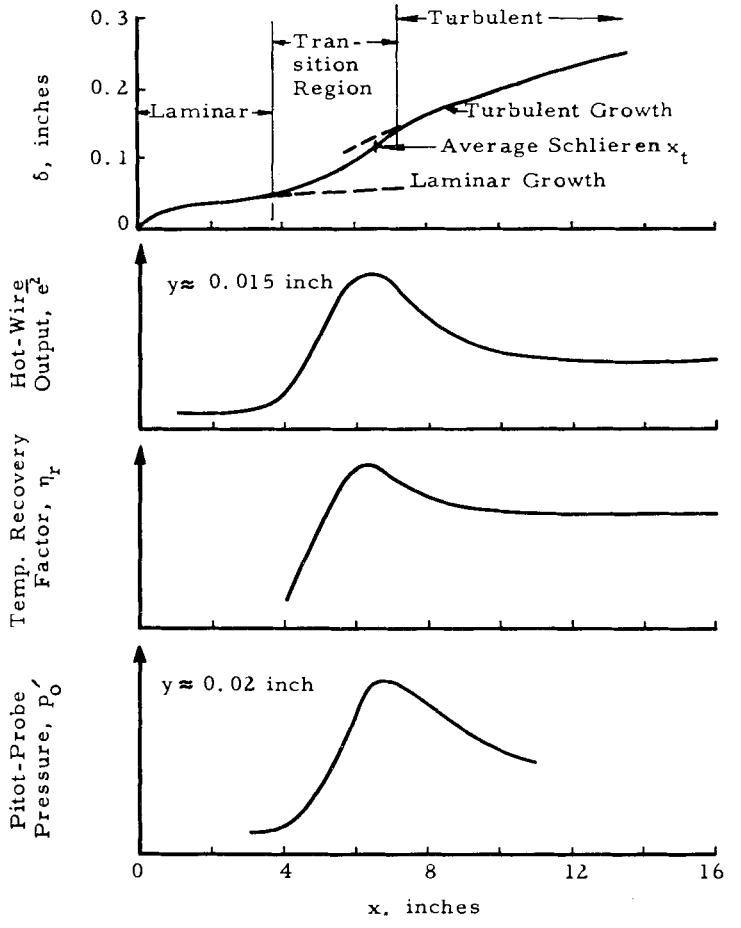

FIGURE 5. Comparison of methods of transition detection for $M_\infty = 3{\cdot}5$, $b = 0{\cdot}003$ in., $U_\infty/\nu_\infty = 270{,}000$/in.

Transition data and extent of transition region

Measurements of transition locations by the previously described methods were completed for two leading edge thicknesses, $b = 0{\cdot}003$ and $0{\cdot}008$ in., for $M_\infty = 3$ to 5, and for $b = 0{\cdot}002$ in. at $M_\infty = 8$. These data permit study of the extent of the transition region as influenced by the variables present. Examples are shown in figures 8 and 9, the more plentiful $M_\infty = 4{\cdot}5$ data being typical of the lower Mach numbers.

Determination of transition location from wall-temperature distribution always made use of data corresponding to a condition of equilibrium wall temperature at all Mach numbers. However, since it was very inconvenient to establish this condition for all testing, transition locations determined by other

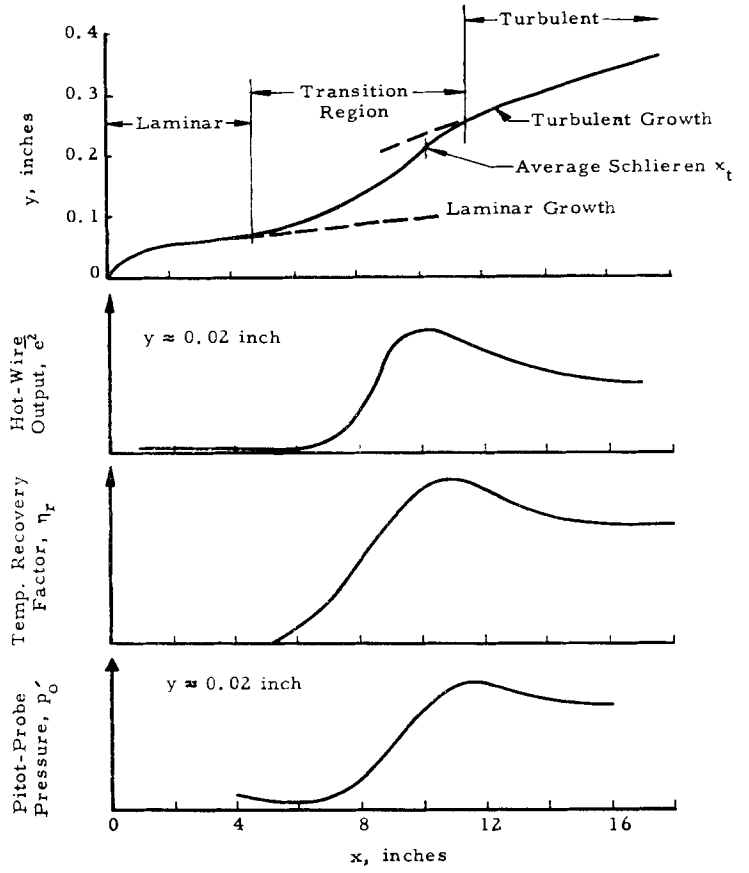

FIGURE 6. Comparison of methods of transition detection for $M_\infty = 5$, $b = 0{\cdot}003$ in., $U_\infty/\nu_\infty = 280{,}000$/in.

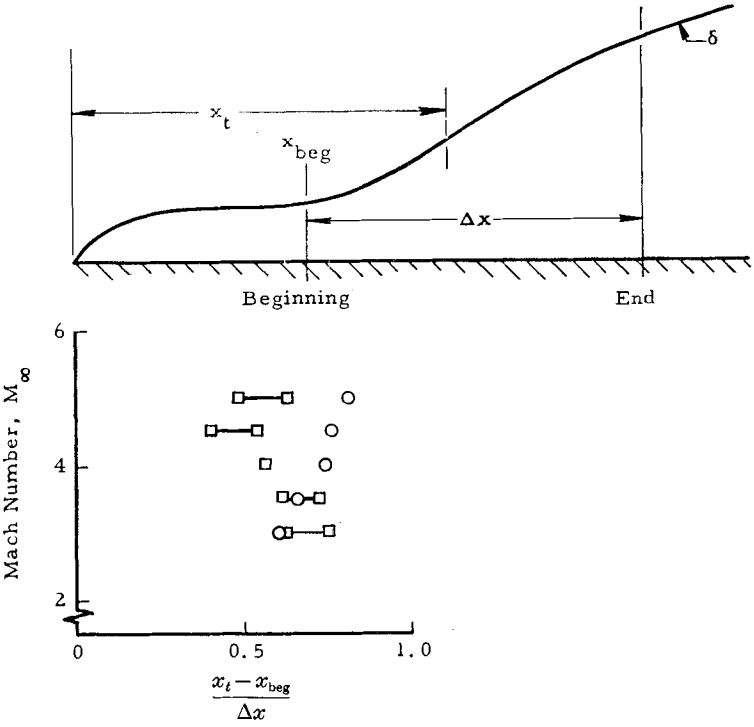

FIGURE 7. Similarity of transition region. Method of detection: ○, maximum hot-wire output, $\overline{e^2}$ or maximum T_w; □, Schlieren.

methods in the $M_\infty = 3$ to 5 range correspond to slightly non-equilibrium heat-transfer conditions. At Mach numbers of 3 to 5, the wall temperature was between zero and 7 % greater than its adiabatic recovery value, and tests indicated no discernible effect on transition location. At Mach number 8, radiation from model

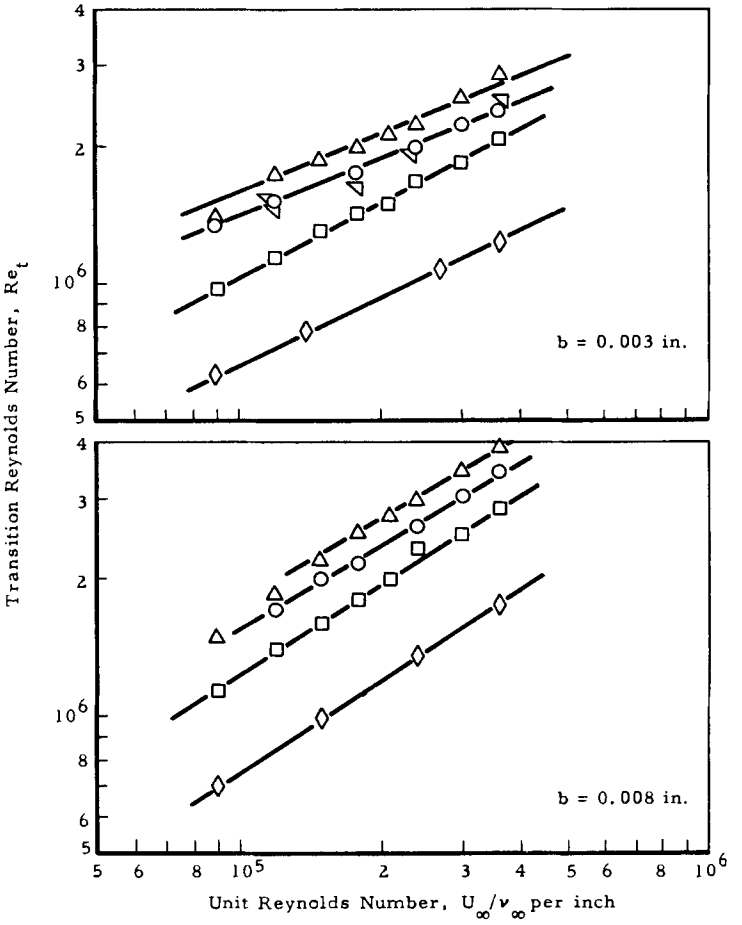

FIGURE 8. Transition results at $M_\infty = 4{\cdot}5$ for $b = 0{\cdot}003$ in. and $0{\cdot}008$ in. ○, Maximum $\overline{e^2}$; △, maximum p_0'; □, Schlieren; ▽, maximum T_w; ◇, limit of laminar δ.

to surroundings apparently established an equilibrium wall temperature less than adiabatic recovery. The ratio T_w/T_∞ was 10, whereas the theoretical adiabatic recovery value would have been 12.

The influence of Mach number on the magnitude of the transition Reynolds number and the extent of the transition region is presented in figure 10. The tendency of transition Reynolds numbers to increase with increasing Mach number (U/ν constant) in the hypersonic régime has been observed before.

Study of these data indicates that the transition region, when defined in terms of a transition-zone Reynolds number ($Re_{\Delta x} = U_\infty \Delta x/\nu_\infty$), depends little on the unit Reynolds number and leading-edge geometry, i.e.

$$Re_{\Delta x} = f(Re_t, M_\infty), \tag{1}$$

as shown in figure 11. The transition zone Reynolds number, $Re_{\Delta x}$, is plotted as a function of Reynolds number based on distance to the end of transition, $(Re_t)_{end}$, because of the better experimental definition of the end as compared to the beginning of transition at supersonic and hypersonic speeds. Also included in figure 11 are subsonic data from Silverstein & Becker (1938), Schubauer & Skramstad (1948), Bennett (1953), Feindt (1956), and Smith & Clutter (1957).

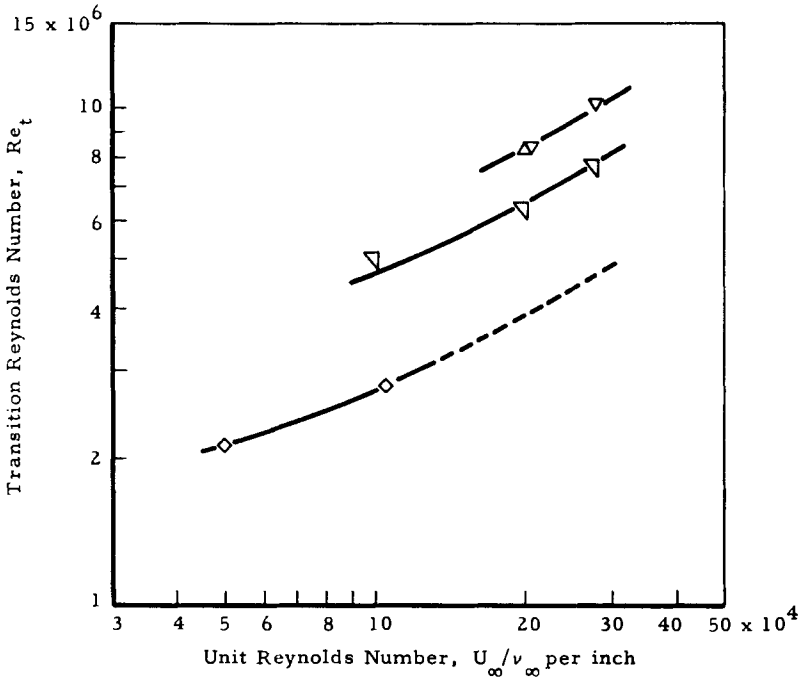

FIGURE 9. Transition results at $M_\infty = 8$ for $b = 0{\cdot}002$ in. (VKF hollow cylinder, $\theta = 11{\cdot}5°$). $\diamondsuit$, Deviation from laminar δ growth; $\triangledown$, (T_w/T_0) maximum; $\triangle$, beginning of turbulent δ growth; $\triangledown$, beginning of constant (T_w/T_0).

These subsonic data include data taken under the influence of pressure gradients and varying turbulence levels in the free stream, yet they seem to fit in very well. The supersonic data are from Coles's (1953) flat-plate data or the hollow cylinders of the present study. Although a singificant increase in $Re_{\Delta x}$ is associated with increasing Mach number, the rate of increase of Δx with Mach number is not as great as the rate of increase in the boundary-layer thickness. Based on δ at the beginning of transition, we find that

$$\text{for} \quad M_\infty \to 0, \quad \Delta x/\delta \approx 150,$$

and

$$\text{for} \quad M_\infty \geqslant 4, \quad \Delta x/\delta \approx 80.$$

5. Distribution of fluctuations and the critical layer

Boundary-layer surveys with the hot-wire were made for several Mach numbers, unit Reynolds numbers, and leading-edge thicknesses, both with and without surface roughness. All of the surveys obtained with a smooth surface had

the same characteristic pattern. The influence of a change in leading-edge thickness at $M_\infty = 5$ and $U_\infty/\nu_\infty = 280{,}000$ per inch is illustrated in figure 12. The influence of the increased leading-edge thickness on the location and extent of the transition region may be noted; otherwise the pattern is the same.

The flow region near the leading edge and immediately downstream was studied in some detail. This work had a twofold purpose: (*a*) the possibility of a leading-edge separation bubble was considered, and (*b*) it was desired to define better the stratification of fluctuations very near the leading edge and their variation with Mach number.

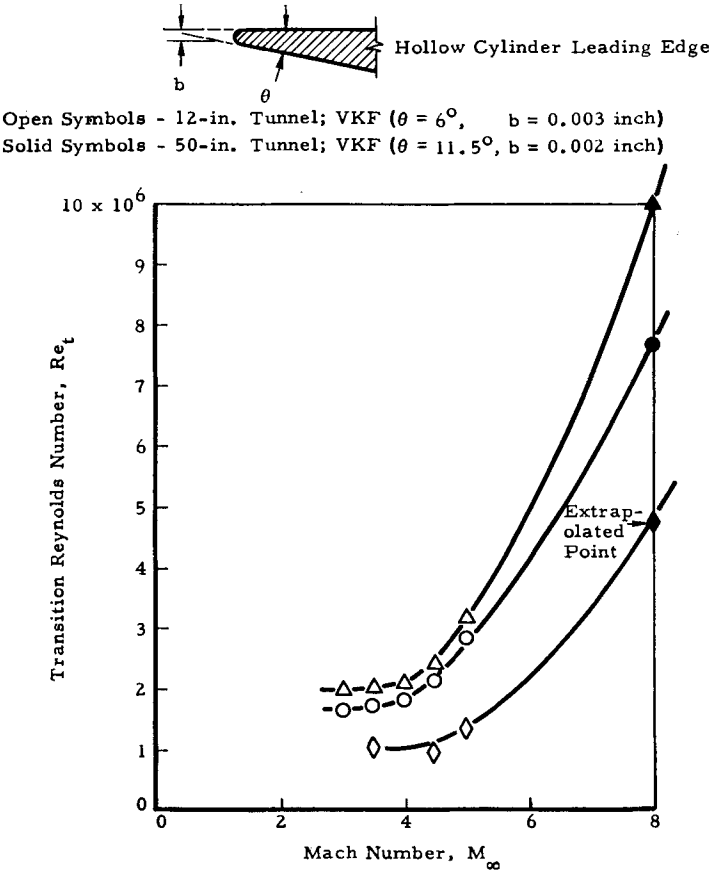

FIGURE 10. Influence of Mach number on transition Reynolds number for $U_\infty/\nu_\infty = 280{,}000/$ in. ○, $(T_w/T_0)_{max}$ or $(\overline{e^2})_{max}$ as $y \to 0$; △, end of transition (beginning of turbulent δ growth), ◇, beginning of transition (limit of laminar δ growth).

Regarding the first objective, considerable time was spent in probing the leading-edge vicinity with hot-wire and pressure probes. No evidence of flow separation could be detected. It was therefore concluded that any leading-edge separation bubbles were quite small compared to probe size if they existed.

Typical results related to the second objective are presented in figure 13. The fluctuations were found to exist quite close to the leading-edge. Also evident here are the extremely sharp vertical gradients of fluctuation energy existing within

the laminar boundary layer. This is seen in both the diagram of isolines of $\overline{e^2}$ and the cross-plot of $\overline{e^2}$ *vs* height y. The cross-plot of hot-wire output, $\overline{e^2}$ *vs* y, was obtained from constant-current operation of the hot-wire and hence contains the effect of marked variation in sensitivity across the boundary layer. Since the sensitivity of the hot-wire to all fluctuations decreases quite rapidly as the wire is moved from the model surface towards the free stream, it can be seen that the

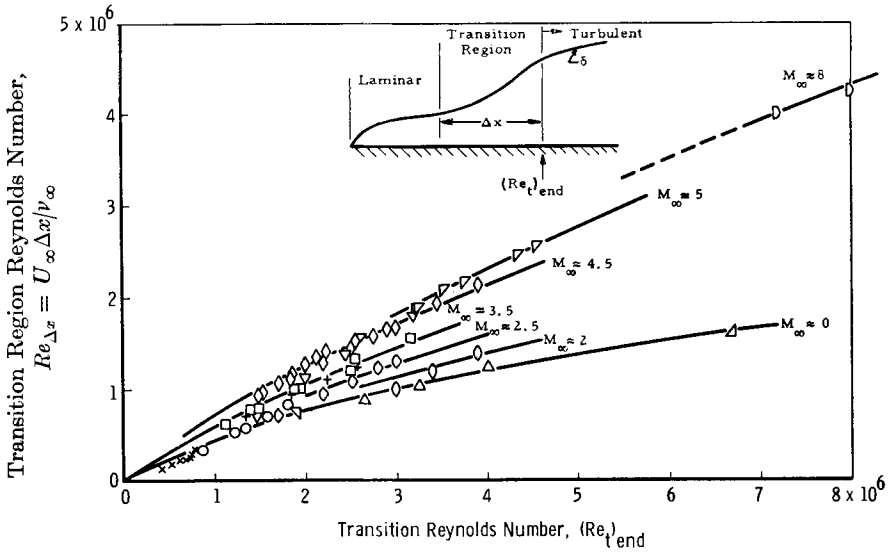

FIGURE 11. Reynolds numbers of the transition region.

Symbol	M_∞	Reference
◹	≈0	Bennett (1953)
○	≈0	Silverstein & Becker (1938)
△	≈0	Schubauer & Skramstad (1948)
×	≈0	Feindt (1956)
◿	≈0	Smith & Clutter (1957)
◊	1·97	Coles (1953)
⬭	2·57	Coles (1953)
+	3·70	Coles (1953)
▽	4·54	Coles (1953)
□	3·5	Potter & Whitfield (1960), VKF
◇	4·5	Potter & Whitfield (1960), VKF
◸	5	Potter & Whitfield (1960), VKF
D	8	Potter & Whitfield (1960), VKF

fluctuation energy concentration in the critical layer is very pronounced. Laufer & Vrebalovich (1958) have shown in a classic experimental treatment of the stability of a supersonic laminar boundary layer that this critical layer is the result of disturbances which have developed into a wave motion with a definite wave velocity and amplitude variation, as expected from stability theory. A similar result has been shown by Demetriades (1958) for a laminar hypersonic boundary layer.

An interesting result of the present experimental study of the critical layer for various unit Reynolds numbers, leading-edge thicknesses, and Mach numbers is

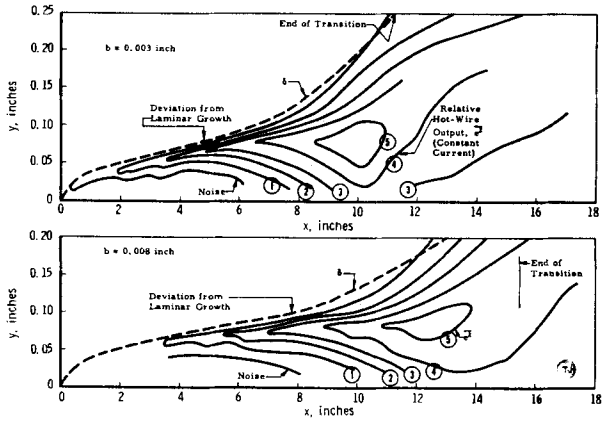

FIGURE 12. Comparison of isolines of hot-wire output for $b = 0{\cdot}003$ in. and $0{\cdot}008$ in. at $M_\infty = 5$, $U_\infty/\nu_\infty = 280{,}000$/in.

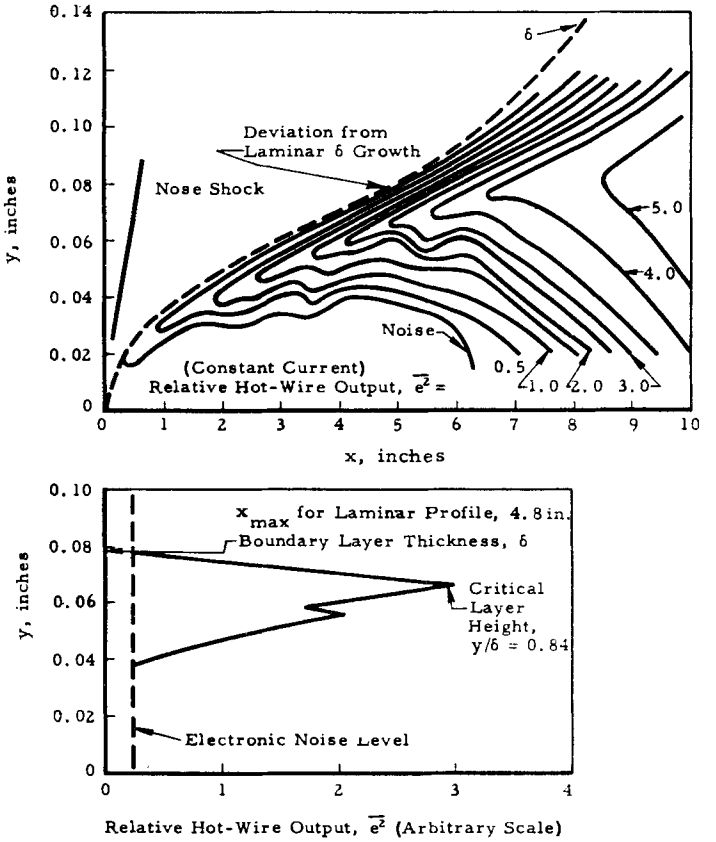

FIGURE 13. Hot-wire output near leading edge for $b = 0{\cdot}003$ in., $M_\infty = 5$ and $U_\infty/\nu_\infty = 280{,}000$/in.

that the height of the critical layer can be represented reasonably well in terms of boundary-layer thicknesses and Mach number, i.e.

$$y_c/\delta = f(M_\infty). \tag{2}$$

This relationship is given by figure 14, where the present data are compared with subsonic data from Klebanoff & Tidstrom (1959) and the earlier mentioned data from Laufer & Vrebalovich and Demetriades.

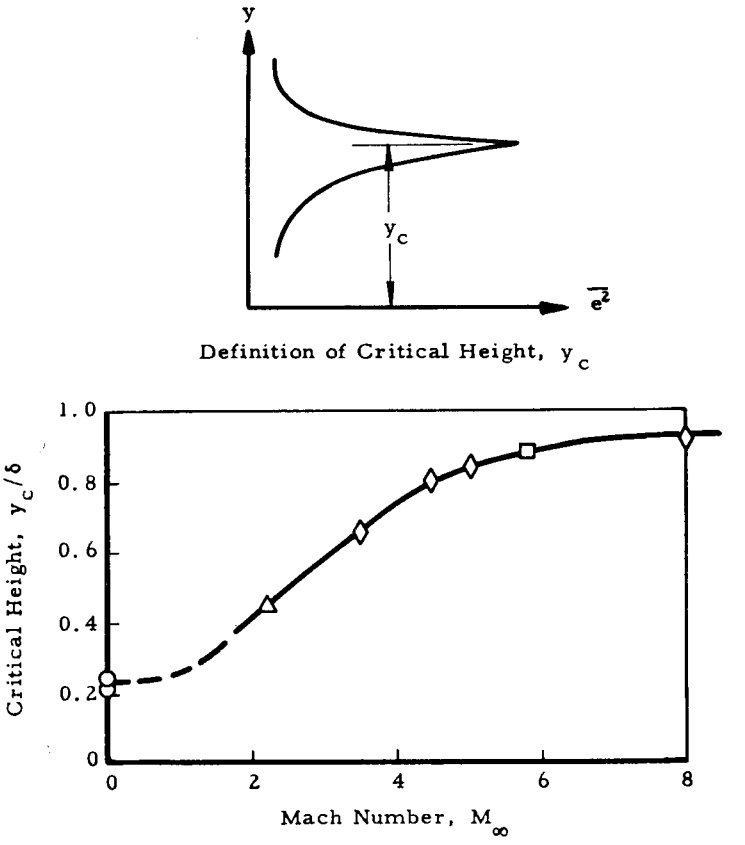

FIGURE 14. Critical layer height as a function of Mach number. ○, Klebanoff & Tidstrom (1959); △, Laufer & Vrebalovich (1958); □, Demetriades (1958); ◇, Potter & Whitfield (1960), VKF.

The origin of the natural disturbances in the boundary layer is, of course, a question of considerable interest. The present results infer, as do the results of Laufer & Vrebalovich, that these disturbances exist all the way forward to the leading edge. The possibility of significant leading-edge separation bubbles has been eliminated. However, both of these experiments were conducted on two-dimensional models with sharp leading-edges. A brief experiment was conducted to examine the possibility that these disturbances might be produced only by the sharp two-dimensional leading edge. The front of the 3 in. diam. hollow cylinder was closed with a smooth nose to form a body of revolution. This nose was

constructed in the form of a cone-cylinder. The cone apex was rounded off with a spherical radius of 0·5 in. tangent to the cone and the cone-cylinder junction was faired smooth with approximately a 3 in. radius; thus no sharp edges existed. The results of a hot-wire survey at constant x are shown in figure 15. The reduced local unit Reynolds numbers produced by the strong nose shock resulted in laminar flow over the available test length of this model. These surveys were taken at an aft station for easier detection of a critical layer. Evidence of a critical layer is clear.

Laufer & Vrebalovich suggested that free-stream turbulence, acting as a forcing function, causes an interaction between the shock wave and the boundary layer, and this in turn produces disturbances in the boundary layer. Having determined that the disturbances and their distribution in the boundary layer are not peculiar to very sharp leading edges nor due to separation at the leading edge, the present study indirectly supports their hypothesis.

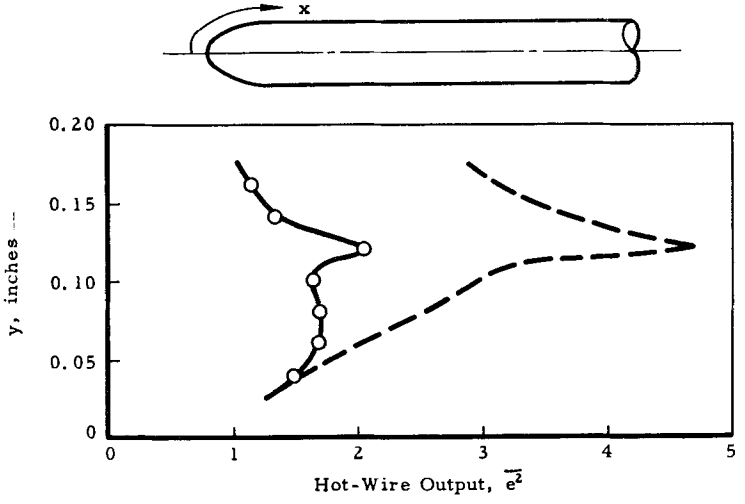

FIGURE 15. Hot-wire output in boundary layer of a smooth-nosed body of revolution. $M_\infty = 4{\cdot}5$, $x = 18$ in., $U_\infty/\nu_\infty = 280{,}000$/in.; ○, constant hot-wire current; ———, estimated for constant wire temperature.

An example of surveys behind roughness elements ($\frac{1}{16}$ in. diam. spheres) of a height greater than the undisturbed boundary-layer thickness is shown in figure 16. For comparison, the smooth surface case also is shown. Such cases as this represent the only departures observed from the characteristic pattern of isolines shown for the smooth model. These data suggest that similarity of the natural transition process is not maintained behind large roughness elements. This in turn suggests that measurements should be made in a region well removed from the roughness element if it is desired to simulate turbulent flow due to natural transition. It should also be noted that large roughness elements can produce flow distortions extending outside the natural boundary layer and persisting well downstream of the roughness location. When such large roughness elements are used, the distortion of the flow external to the boundary layer may be so great as to affect quantities normally not influenced by the boundary layer.

Since large roughness usually is required by locally hypersonic Mach numbers on adiabatic walls, tripping the boundary layer without undesirable side effects is difficult.

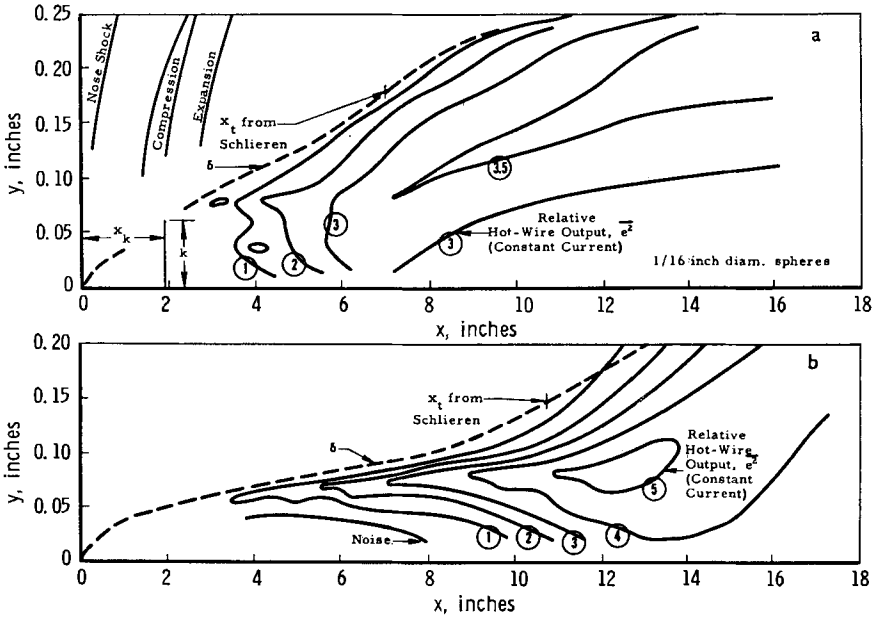

FIGURE 16. Comparison of hot-wire outputs with and without surface roughness, $M_\infty = 5$, $b = 0{\cdot}008$ in., $U_\infty/\nu_\infty = 280{,}000$/in. (*a*) $\frac{1}{16}$ in. diam. spheres, $k = 0{\cdot}067$ in., $x_k = 1{\cdot}9$ in.; (*b*) smooth.

6. The effect of leading edge geometry

Bluntness at the leading edge of an aerodynamic body has an important effect on transition and has been studied by several investigators. Brinich & Sands (1957) have published one of the more recent experimental studies of leading-edge bluntness. Their studies were conducted with a stream Mach number of 3·1.

Bertram (1957) suggested that the frequently observed, sometimes marked, increase in Re_t with increasing U_∞/ν_∞ in supersonic flow could be due to the finite leading edges always present. Bertram plotted Brinich & Sands's data in the form of transition Reynolds number ($Re_t = U_\infty x_t/\nu_\infty$) *vs* bluntness Reynolds number ($Re_b = U_\infty b/\nu_\infty$, where b = leading-edge thickness) to illustrate the similar influence of increasing U_∞/ν_∞ or increasing Re_b on the transition Reynolds number, Re_t. Examination of these plots and other data reveal a systematic behaviour not accounted for by this method of correlation.

The present studies were undertaken to extend available data on the effects of small degrees of leading-edge bluntness to higher Mach numbers and to examine closely the possible relationships between bluntness effects and unit Reynolds number effects. The present experimental studies were conducted with a hollow cylinder model. The results and analysis are based on transition locations derived from the maximum hot-wire signal, $\overline{e^2}$, with the probe traversed near the surface. This has been shown to be directly compatible with transition locations derived from maximum surface temperatures, as used by Brinich & Sands.

Attempts to correlate the present data in terms of a ratio of transition locations revealed systematic deviations depending on how the variation in Re_b was obtained. The transition distance ratio was observed to be a function of U_∞/ν_∞ and b as well as of their product, i.e.

$$(x_t)_b/(x_t)_{b\to 0} = f(U_\infty/\nu_\infty, b). \tag{3}$$

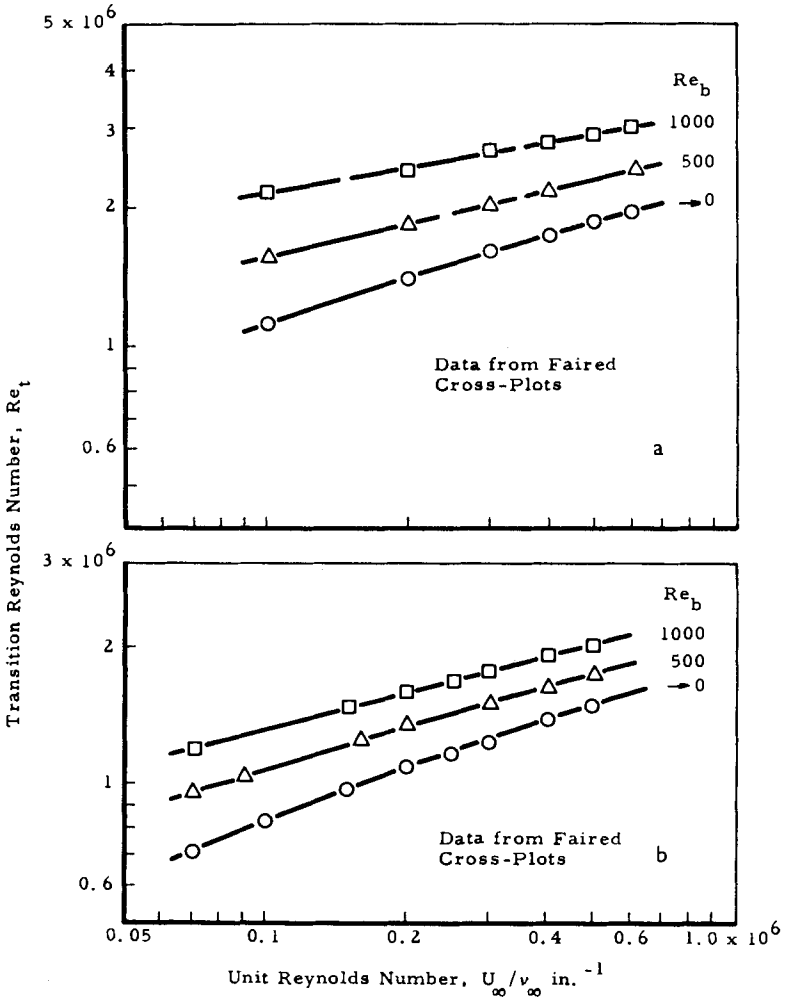

FIGURE 17. Unit Reynolds number influence for various bluntness Reynolds numbers. (*a*) NASA, Brinich & Sands (1957), $M_\infty = 3{\cdot}1, \theta = 15°$; (*b*) VKF, Potter & Whitfield (1960), $M_\infty = 3{\cdot}0, \theta = 6°$.

A study of Brinich & Sands's data for slight degrees of bluntness also reveals small but similar effects. This can be illustrated by cross-plotting the data *vs* U_∞/ν_∞ with Re_b as a parameter. Such cross-plots are shown in figure 17. These curves are plotted in log-log co-ordinates, and the curves are observed to be slightly convergent as U_∞/ν_∞ increases rather than the parallel curves required for constant ratios of transition distances.

Regarding these cross-plots with Re_b as a parameter, two other trends of significance may be noted: (1) Re_t increases with increasing U_∞/ν_∞ for Re_b = const. and (2) there is a marked difference in the magnitude of Re_t between the two sets of data. The first point provides the answer to one of the questions of interest—namely, is the unit Reynolds number effect due entirely to bluntness? Clearly it is not. This and the second point will be discussed later.

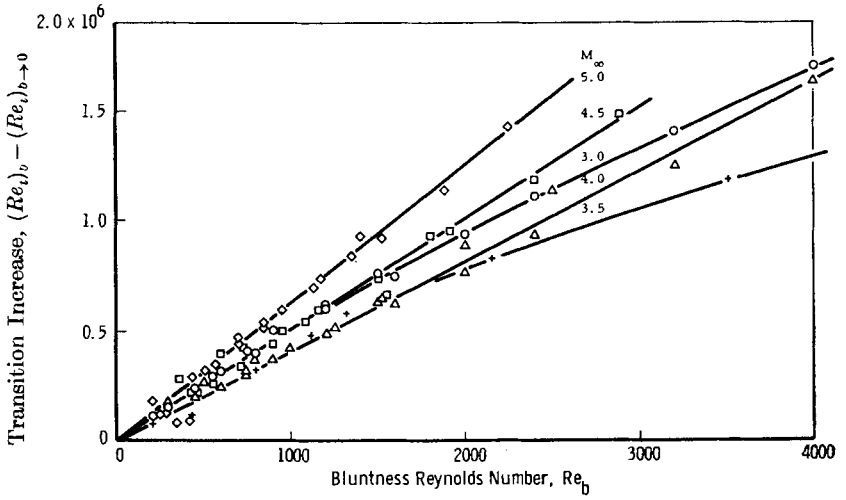

FIGURE 18. Transition Reynolds number increase due to bluntness Reynolds number increase. ○, $M_\infty = 3{\cdot}0$; +, $M_\infty = 3{\cdot}5$; △, $M_\infty = 4{\cdot}0$; □, $M_\infty = 4{\cdot}5$; ◇, $M_\infty = 5{\cdot}0$. (VKF, Potter & Whitfield 1960.)

A close inspection of figure 17 indicates, for a given set of data, a nearly constant incremental change in Re_t for a given increase in Re_b. This suggests a relationship of the form

$$(Re_t)_b - (Re_t)_{b\to 0} = f(Re_b). \tag{4}$$

The VKF data are presented in figure 18 in this manner. The correlation is seen to be quite reasonable for the small bluntness Reynolds numbers of the present study. The indicated influence of Mach number is surprising since a decreasing influence of bluntness is noted from $M_\infty = 3$ to 3·5 as opposed to an increasing influence for $M_\infty > 3{\cdot}5$. The later comparison of these data with other data will indicate an interrelationship of factors influencing these results; hence the interrelation of Mach number and bluntness implied by figure 18 is not conclusive.

The data of Brinich & Sands were reduced in a like manner and compared to the present data in figure 19. Brinich & Sands's data for $M_\infty = 3{\cdot}1$ indicate nearly twice the influence of bluntness in comparison with the present data. Two possible reasons for differences in these data are differences in leading-edge geometry noted in figure 19, and the use of different wind tunnels. Comparison of some transition data from a 10 deg. cone in the VKF 12 in. tunnel and transition data from Brinich & Sands on a 10 deg. cone taken during their study of bluntness do not reveal significant differences. However, it was shown in figure 17 that an appreciable difference in the absolute magnitude of Re_t existed between the hollow-cylinder models.

Assuming, for the moment, that similar results would be obtained from the two wind tunnels for a given model, the explanation of these data was sought in the differences in leading-edge geometry. Laufer & Marte (1955) tested a flat plate with a bottom or internal bevel angle of 24 deg. in the Jet Propulsion Laboratory's 20 in. wind tunnel (JPL 20 in.). These results are compared with Brinich & Sands's data and the VKF data in figure 20. Assuming now that three wind tunnels (VKF 12 in. tunnel, NASA Lewis 12 in. tunnel, and JPL 20 in. tunnel) would

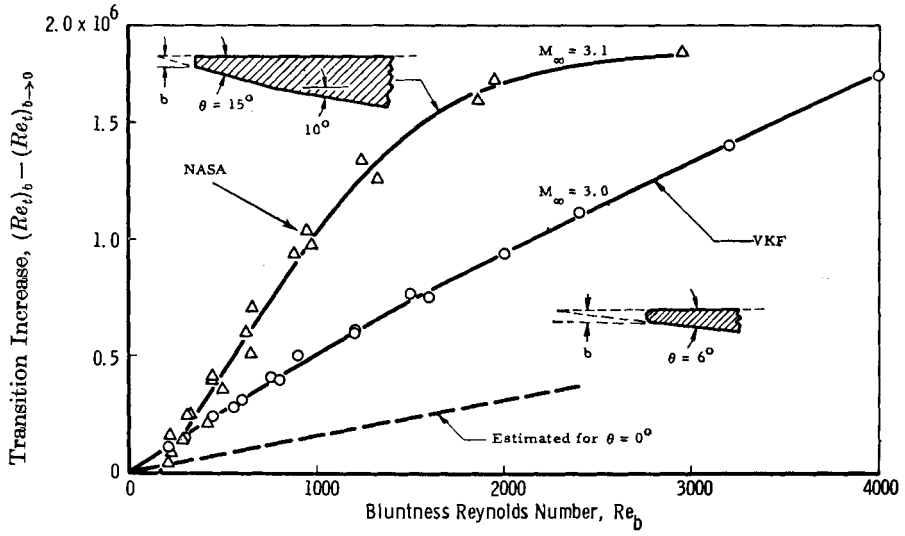

FIGURE 19. Comparison of Brinich & Sands' (1957) NASA data and Potter & Whitfield (1960) VKF data.

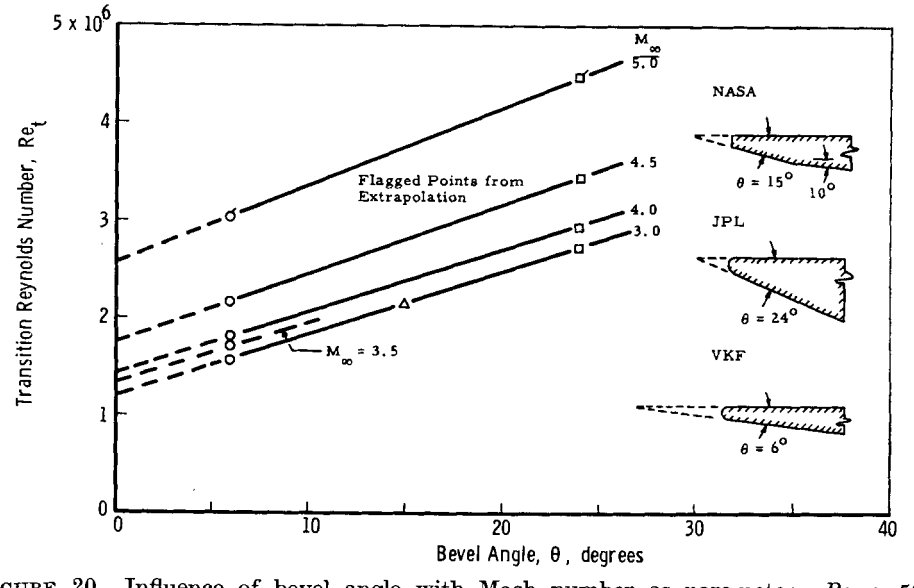

FIGURE 20. Influence of bevel angle with Mach number as parameter. $Re_b \approx 500$, $U_\infty/\nu_\infty \approx 340{,}000$/in. △, NASA, Brinich & Sands (1957); □, JPL–20 in., Laufer & Marte (1955); ○, VKF, Potter & Whitfield (1960).

produce similar results on a given model, a rather strong influence due to the bevel angle appears to be present.

An explanation of the apparent interrelations between bluntness Reynolds number and the bevel angle is not known. However, consideration of the local subsonic flow produced by a finite leading-edge bluntness points to the possibility of an influence of the bevel on the stagnation point location. If such a movement

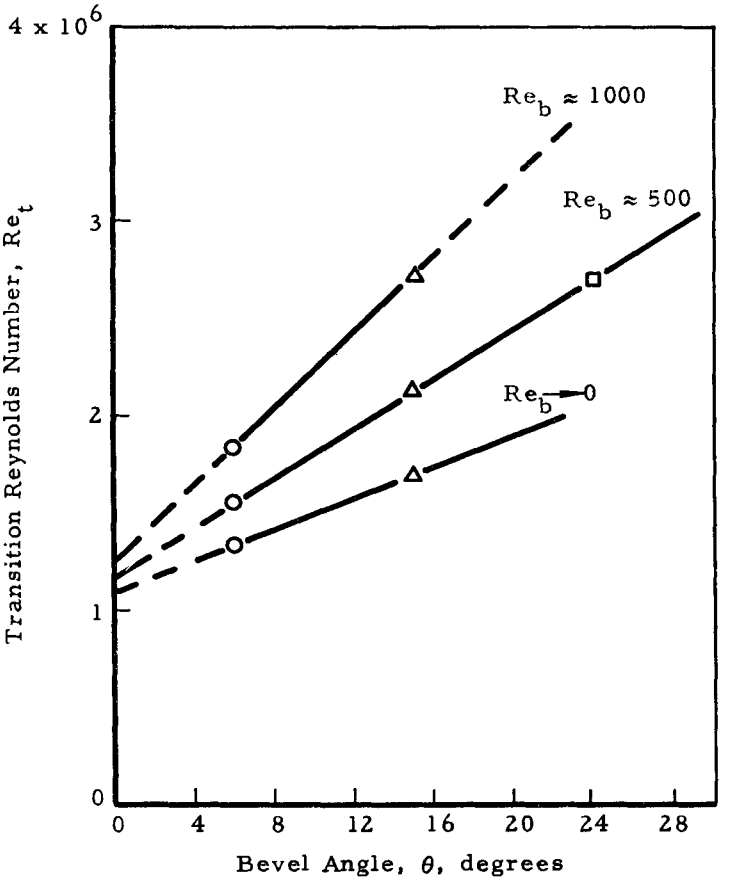

FIGURE 21. Influence of bevel angle with bluntness Reynolds number as a parameter. $M_\infty \approx 3$, $U_\infty/\nu_\infty = 340{,}000$/in. △, NASA, Brinich & Sands (1957); □, JPL, Laufer & Marte (1955); ○, VKF, Potter & Whitfield (1960).

occurs, then a change in the shock-induced shear layer adjacent to the model surface may occur. Leading-edge vibrations are another possible source of the effect of the bevel angle. However, it seems unlikely that the influences on such vibrations due to changing U_∞/ν_∞ or tunnel density level would be almost exactly the same as varying the physical leading-edge thickness to produce a given change in the bluntness Reynolds number, Re_b. This latter possibility is discounted for lack of proof at this time, and the Re_t values extrapolated to $\theta = b = 0$ are referred to as the 'aerodynamically'-flat plate data.

Based on the assumption that the three sets of data are directly comparable, sufficient information is at hand to estimate the combined effects of leading-edge

bluntness and the bevel angle for $M_\infty \approx 3$. A typical plot for $U_\infty/\nu_\infty = \text{const.}$ with Re_b as a parameter is shown in figure 21. Such cross-plots for other U_∞/ν_∞ values indicate that although the level of all the curves increases as U_∞/ν_∞ increases, the interrelation between Re_b and θ is substantially independent of U_∞/ν_∞. The data of figure 21 indicate that

$$(Re_t)_{\theta,b} = (Re_t)_{\theta=0,b=0} + f(Re_b, \theta). \tag{5}$$

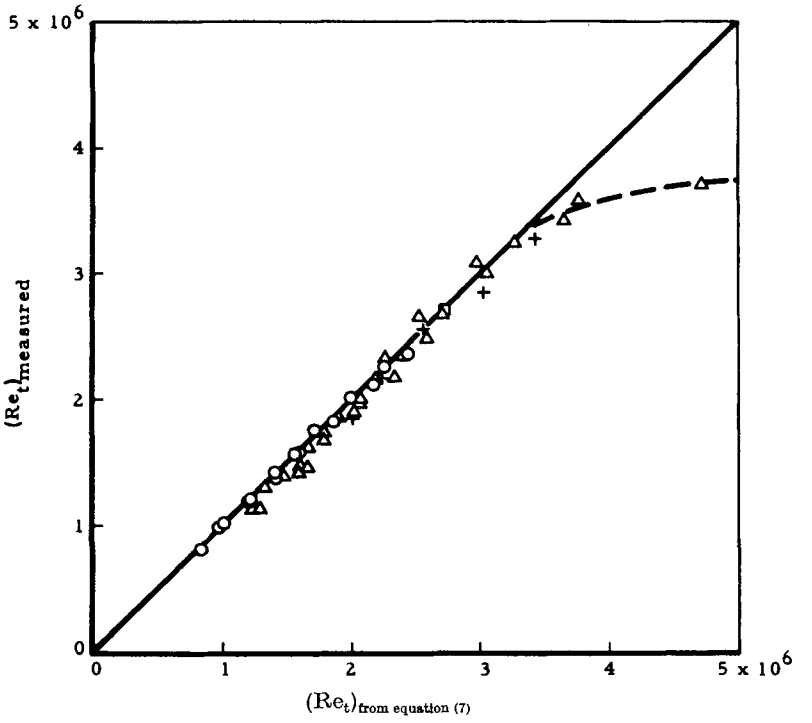

FIGURE 22. Comparison of estimated and measured transition Reynolds numbers for $M_\infty \approx 3$. $Re_t = (Re_t)_{b=0,\theta=0} + 160\,Re_b + 36500\theta + 55 Re_b\theta$. ○, VKF, $\theta = 6°$ Potter & Whitfield (1960); △, NASA (Lewis), $\theta = 15°$, Brinich & Sands (1957); □, JPL, $\theta = 24°$, Laufer & Marte (1955); +, NASA (Ames), $\theta = 8°$, Chapman, Kuehn & Larson (1957).

Using linear relationships for the case of small degrees of bluntness, an empirical relation of the following form was considered:

$$(Re_t)_{\theta,b} = (Re_t)_{\theta=0,b=0} + \frac{\partial Re_t}{\partial Re_b} Re_b + \frac{\partial Re_t}{\partial \theta}\theta + \frac{\partial^2 Re_t}{\partial Re_b \partial \theta} Re_b\theta. \tag{6}$$

From figure 21 and other similar plots, these constants were evaluated and it was found that

$$(Re_t)_{\theta,b} = (Re_t)_{\theta=0,b=0} + 160 Re_b + 36500\theta + 55 Re_b\theta, \tag{7}$$

where θ is in degrees. The experimental data used in this analysis may be summarized by comparison with equation (7). This comparison is given in figure 22 for many U_∞/ν_∞ and b values. The use of linear relationships for the effect of Re_b and θ is seen to allow an accurate estimate of Re_t for small nose radii. Also included in figure 22 are data obtained by Chapman, Kuehn & Larson (1957) on a flat plate. These data were not used in the analysis to evaluate the constants in the above relation but are seen to agree quite well with the equation given.

The Re_t values for an aerodynamically-flat plate (i.e. $\theta = b = 0$) at $M_\infty = 3$ are shown in figure 23 with data for other Mach numbers to illustrate the U/ν influence. The measured data for $M_\infty = 3$ to 5 may be extrapolated to correspond to $Re_b = 0$, but there are not sufficient data to perform the extrapolation to $\theta = 0$. The unit Reynolds number influence is found to be present in varying degrees in all the experimental data on figure 23, even in the aerodynamically-flat plate case.

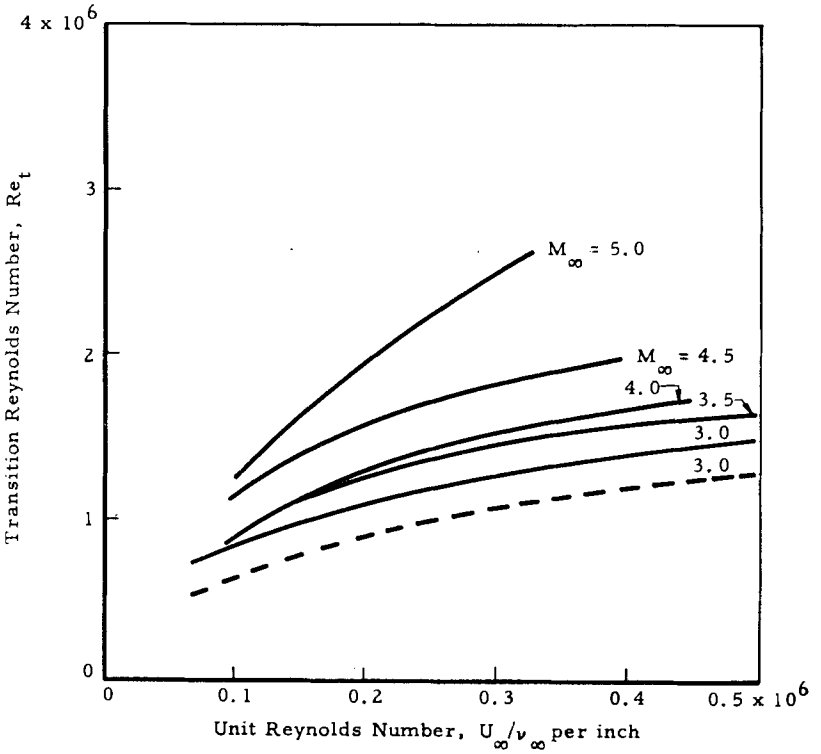

FIGURE 23. Unit Reynolds number effect for various Mach numbers as $Re_b \to 0$. ——, $\theta = 6°$; – – –, $\theta \to 0°$, 'aerodynamically'-flat plate.

The possibility that free-stream or noise-generated turbulence is associated with the unit Reynolds number effect remains (Laufer 1961). Suitable free-flight transition data would help to resolve this question. Although free-flight data showing increasing Re_t with increasing U/ν exist, the data are not complete enough to permit comparison without first making large corrections. Figure 24 shows how available free-flight data on sharp cones compare with wind-tunnel data on cones from figure 25. The flight data have been adjusted to constant Mach number using the experimental data of Laufer & Marte, and the further adjustment to adiabatic wall recovery temperature was based on the experimental data of Van Driest & Boison (1957). Because of the size of these adjustments and data scatter, it would not be safe to accept the apparent compatibility of flight and tunnel data as conclusive.

The analysis of the effect of slight nose bluntness has been based on the assumption that data from the three wind tunnels are directly comparable.

Although it was stated earlier that transition data for cones were available, the discussion of these results was delayed since it was also desired to compare the estimated Re_t for an aerodynamically-flat plate (i.e. $\theta = b = 0$) to Re_t for a sharp cone. Comparison of the test facilities and results obtained for the aerodynamically-flat plate and the cone are shown in figure 25. Fluid properties for this comparison are based on conditions at the outer edge of the boundary layer. Since most of the cone data were available for $M_\delta = 2{\cdot}7$, cone data and the aerodynamically-flat plate data were corrected to $M_\delta = 2{\cdot}7$ using the Mach number effect for transition on a cone found by Laufer & Marte (1955). Data from the JPL 12in. tunnel also are included to illustrate the similarity of the U/ν effect on Re_t for a cone and an

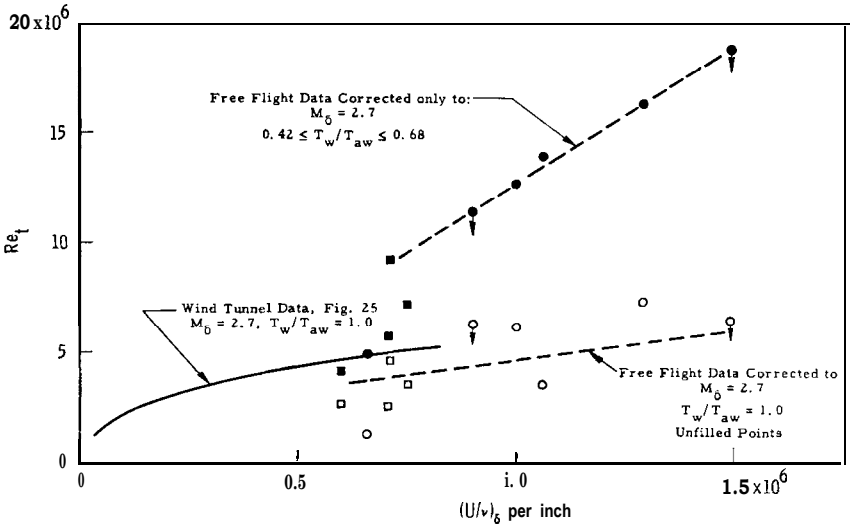

FIGURE 24. Comparison **of boundary-layer transition on cones as measured in free flight and in wind tunnels. ●, Cone angle = 10°, Rumsey & Lee (1956); ⌀⌀, cone angle = 15°, Rumsey & Lee (1958); —, cone angle = 10°,** VKF, Potter & **Whitfield** (1960); ↓ **indicates 'less than'.**

aerodynamically-flat plate. The agreement between the wind tunnels is seen to be reasonable and the factor between Re, on a cone and the aerodynamically-flat plate is approximately 3. This is a significant result and it is interesting to note that Battin & Lin (1950) predicted that the minimum critical Reynolds number of stability theory would be in the same ratio for the cone and plate.

The apparent strong interdependence of factors defining the leading edge of a flat plate or hollow-cylinder model prevents us from drawing conclusions regarding the detailed influence of Mach number on leading edge effects. Hence the influence of Mach number on the aerodynamically-flat plate cannot be precisely evaluated at this time.

7. The effect of surface roughness

Previous studies of this subject have been reported in references too numerous to mention here. Among the more recent and better known is that published by Dryden (1953) who dealt with low-speed flows. He found that the ratio of the

Reynolds numbers of transition with and without roughness, Re_t/Re_{to}, was well represented as a function of k/δ_k^*, the ratio of roughness height to the displacement thickness of the undisturbed boundary layer at the station of roughness. The correlation held only for transition locations, x_t, less than or equal to x_{to} and

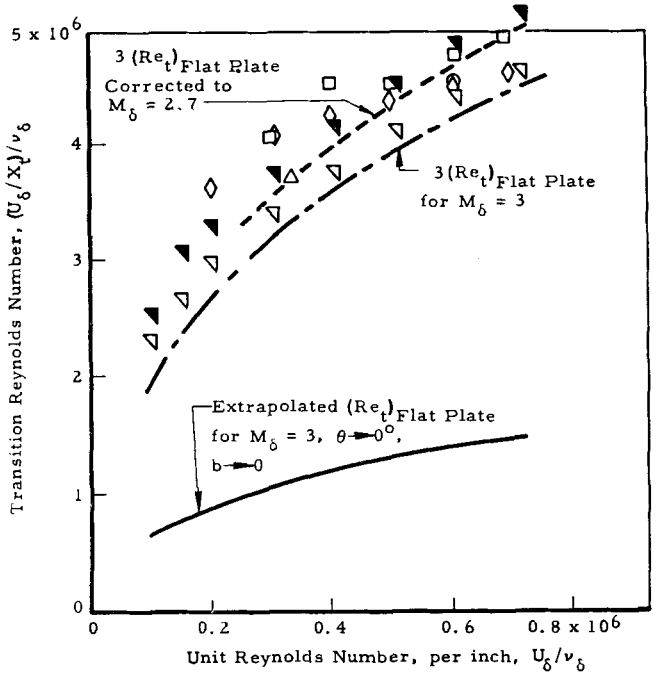

FIGURE 25. Comparison of transition data from various wind tunnels and comparison of flat-plate and cone transition data.

Symbol	Tunnel	Method	M_δ	Remarks	Reference
○	VKF–12 in.	Max. T_w/T_δ	2·7	10° cone	Potter & Whitfield (1960)
△	JPL–20 in.	Max. T_w/T_δ	2·7	5° cone	Laufer & Marte (1955)‡
□	JPL–12 in.	Max. T_w/T_δ	2·7	10° cone	Van Driest & McCauley (1958)
◇	JPL–12 in.	Schlieren	2·7	10° cone	Van Driest & McCauley (1958)
◹	NASA (Lewis 12 in.)	Max. T_w/T_δ	3·0	10° cone	Brinich & Sands (1957)
◥	—	Max. T_w/T_δ	†		

† Corrected to M_δ = 2·7. ‡ From faired curve.

greater than x_k, where x_{to} corresponds to the case of no roughness and x_k is the station where roughness is attached. Figure 26 illustrates some of the nomenclature used in this discussion.

Further experimental testing of Dryden's parameter was reported by Klebanoff, Schubauer & Tidstrom (1955), who found that k/δ_k^* served admirably for single two-dimensional elements in subsonic flow but was totally ineffective as a correlation parameter when the roughness consisted of a single row of spheres.

The latter investigators suggested that the three-dimensional roughness seemed to have little effect on transition when the quantity Re_k was less than some critical value, and that the location of transition moved almost precipitously to a point near the station where roughness was attached when Re_k slightly exceeded this critical value. The parameter Re_k is defined as

$$Re_k = u_k k/\nu_k, \tag{8}$$

where u_k/ν_k is the unit Reynolds number in the undisturbed boundary layer corresponding to conditions at height k and location x_k and k is the height of the roughness.

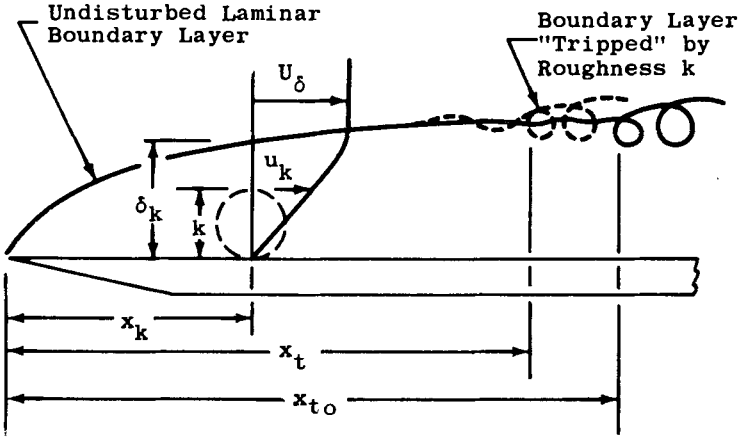

FIGURE 26. Roughness nomenclature.

A critical Reynolds number equivalent to $\sqrt{Re_k}$ appears to have been suggested originally by Schiller (1932). However, the concept of a nearly stepwise shift of transition from its undisturbed location x_{to} to the roughness station x_k was proved erroneous as a general rule by the data of Fage (1943) and numerous later investigators. The more recent view has credited this critical behaviour to three-dimensional roughness, while considering that two-dimensional roughness produces a more gradual effect on the mean location of transition. It will be observed when viewing recent data that even three-dimensional roughness does not always produce an instantaneous shift of x_t.

Tani, Hama & Mituisi (1954) published a paper in which they described a roughness correlation parameter based on G. I. Taylor's parameter for transition caused by free-stream turbulence. This accomplished a correlation of their data for the case of single two-dimensional elements on a flat plate in low-speed flow. Unaware of this work, which was not widely known in the United States, one of the present authors (Potter 1957) undertook to derive a roughness parameter from the Pohlhausen boundary-layer profile parameter after the manner of Taylor's early analysis of free-stream turbulence. Tani *et al.* arrived at their parameter by replacing certain terms in Taylor's parameter by appropriate roughness characteristics. The analysis by Potter was done by setting the problem in functional form and determining empirically the functions from published data. Again, only the single two-dimensional element on a flat plate in low-speed flow

was considered. It was Gibbings (1958) who called attention to the fact that both analyses gave results that could be reduced to identical functional forms and differed only by a constant. This slight difference in the value of the constant was due to the use of different experimental data. Although neither expression was originally given in this form, both can be expressed as

$$(U_\delta k/\nu_\delta)\,(x_t/x_k)^{\frac{1}{2}} = \text{const.}$$

Another interesting point is that the left side of this expression, based on flat-plate flow, is proportional to $(U_\delta x_t/\nu_\delta)^{\frac{1}{2}}\,(k/\delta_k^*)$, where k/δ_k^* is the parameter proposed by Dryden.

It should be noted that Winter, Scott-Wilson & Davies (1954) gave values of $U_\delta k/\nu_\delta$ for wires which would fix transition at the wire location. Their data included cases wherein the free-stream Mach number was as high as three. They recommended $U_\delta k/\nu = 700$ for Mach numbers up to 0·9 from whence $U_\delta k/\nu_\delta$ increased exponentially up to about 5200 at the limit of their data, slightly above $M_\delta = 3$. The scatter of data used to define Re_k was very great, but they were forced to use available results from different models having various pressure distributions.

Smith & Clutter (1957) conducted tests in a low-speed wind tunnel to obtain further data on the effects of roughness. They recommended values of Re_k representing maximum sizes of roughness permissible without appreciable effect on transition location. Later, the same authors (1959, 1960) recommended values of a Reynolds number, Re_k^*, to represent the limits $x_t \to x_{to}$ and $x_t \to x_k$. This Reynolds number is defined as

$$Re_k^* = a^* k/\nu^*, \tag{9}$$

where ν^* is based on T^* and p_δ, the superscript * denoting sonic conditions. Smith & Clutter suggested that Re_k^* must exceed approximately 100 for roughness to have effect in very low-speed flows, and approximately 300 to 400 in flows where compressibility effects are important. In order to bring x_t near x_k, they suggested that $Re_k^* \simeq 400$ to 800 for all Mach numbers for both wire and spherical roughness elements. In order to make Re_k^* for very low-speed flow fall in this range they had to define it as $2Re_k$. Gibbings (1958) recently has given yet another criterion for the occurrence of transition at a wire roughness.

At this point it seems appropriate to remark on the emergence of either $U_\delta k/\nu_\delta$ or $u_k k/\nu_k$ in many analyses, even when the starting-points of the analyses appeared completely different. The former parameter is independent of roughness location when $dp/dx = 0$, but the second form of Reynolds number, which we denote by Re_k, is a function of position of roughness as well as height. Therefore the writers have chosen to use a roughness-effectiveness parameter, Re_k', which was derived from Re_k by a modification to be described.

By modification of Re_k it is hoped to account more adequately for the complicated process occurring when a partially supersonic shear flow encounters a roughness element. Smith & Clutter have suggested reducing Re_k to Re_k^* as given by equation (9). This is based on the assumption that sonic flow will always exist near the top of a roughness element when M_k exceeds unity, and may be expressed as

$$Re_k^* = (Re_k/M_k)\,\{[\tfrac{1}{2}(\gamma+1)]/[1+\tfrac{1}{2}(\gamma-1)\,M_k^2]\}^{0\cdot5+\omega}, \tag{10}$$

where it is assumed that

$$T_0 = \text{const.}, \quad p_k = p^* = p, \quad \rho^* = \rho_k(T_k/T^*), \quad \mu^* = \mu_k(T^*/T_k)^\omega.$$

The present authors have investigated yet another approach which is based on the use of a form of Reynolds number to represent the degree of disturbance introduced by roughness. However, this attempt formulates the parameter so that it more nearly reflects the state of affairs downstream of the roughness in the disturbed flow. Toward this end, the results of Chapman *et al.* (1957) are used to estimate the plateau conditions, $(\ )_p$, near a two-dimensional step when $M_k > 1$. A Reynolds number†

$$Re'_k = Re_k(u_p/u_k)\,(\rho_p/\rho_k)\,(\mu_k/\mu_p) = u_p k/\nu_p \tag{11}$$

is considered to represent conditions at the roughness. If

$$p_k = p_\delta \quad \text{and} \quad \mu_p = \mu_k(T_p/T_k)^\omega,$$

(11) may be written as

$$Re'_k = Re_k(M_p/M_k)\,(p_p/p_\delta)\,(T_k/T_w)^{0\cdot5+\omega}. \tag{12}$$

Realizing that the fluid generally will expand and then compress again in flowing downstream from the top of the roughness, with a great deal of mixing in the wake, (12) must remain a rather idealized representation. In an earlier report, the present authors (1960) noted that the product of Mach number and pressure terms in (12) is nearly unity. For cases where the roughness element is close to the wall, it would appear that wall temperature, T_w, should dominate the temperature-dependent quantities in the wake of the roughness. Therefore, it is suggested that the parameter representing the disturbance imposed on the flow leaving conventional roughness elements be defined as

$$Re'_k = Re_k(T_k/T_w)^{0\cdot5+\omega}. \tag{13}$$

For an insulated wall and Prandtl number of unity, (13) reduces to

$$Re'_k/Re_k = \{1 + \tfrac{1}{2}(\gamma-1)\,M_k^2\}^{-(0\cdot5+\omega)}. \tag{14}$$

Equation (13) may be written without Re_k as follows:

$$Re'_k = k\left(\frac{U_\delta}{\nu_\delta}\right)\left(\frac{u_k}{U_\delta}\right)\left(\frac{T_\delta}{T_k}\right)^{0\cdot5}\left(\frac{T_\delta}{T_w}\right)^{0\cdot5+\omega}, \tag{15}$$

or

$$Re'_k = k\left(\frac{U_\delta}{\nu_\delta}\right)\left(\frac{M_k}{M_\delta}\right)\left(\frac{T_\delta}{T_w}\right)^{0\cdot5}. \tag{16}$$

If T_w = adiabatic recovery temperature, (15) becomes

$$Re'_k = \frac{k(U_\delta/\nu_\delta)\,(u_k/U_\delta)\,(T_\delta/T_k)^{0\cdot5}}{[1+\tfrac{1}{2}(\gamma-1)\,\eta_r\,M_\delta^2]^{0\cdot5+\omega}}. \tag{17}$$

Two main features of the present definition of the roughness Reynolds number may be noted. First, it is apparent that Re'_k decreases rapidly with Mach number

† For bodies with walls at adiabatic recovery temperature it is easiest to calculate Re'_k by first obtaining Re_k, u_k, and T_k from Braslow & Knox (1958). Thus Re'_k is often expressed in terms of Re_k in this discussion.

if the wall is at adiabatic recovery temperature, $k(U_\delta/\nu_\delta)$ is constant, and x_k is constant. On the other hand, Re'_k increases rapidly as wall temperature is lowered with other factors remaining constant. In incompressible or low Mach number flow over insulated walls Re'_k and Re_k are equal.

Continuing toward formulation of a correlation procedure, it is suggested that a suitably general term representing location of transition is the Reynolds number based on boundary-layer thickness at transition. In order to eliminate extraneous factors as far as possible, the transition Reynolds number may be divided by its corresponding value when $k = 0$ at the same unit Reynolds number. When $dp/dx = 0$, this ratio is $(x_t/x_{to})^{\frac{1}{2}}$. After lengthy study of experimental data, the

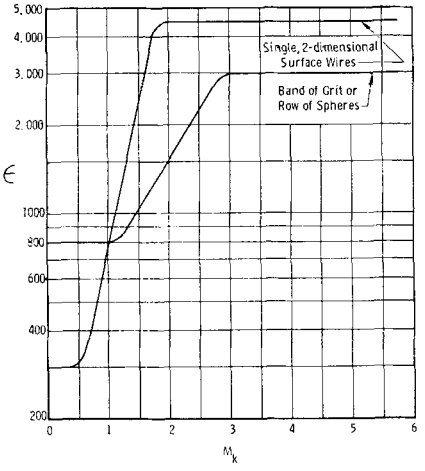

FIGURE 27. Approximate variation of ϵ with M_k for typical roughness.

following parameter representing relative position of transition for all flows with $dp/dx = 0$ was selected: $(x_t/x_{to})^{\frac{1}{2}} - (x_k/x_{to})^{\frac{1}{2}}\,(Re'_k/\epsilon)$.

The quantity which we denote by ϵ represents the value of Re'_k where $x_t \approx x_k$. The 'position' parameter is confined between values of zero and unity, and obviously is designed for the case $x_k < x_t < x_{to}$. The ratio Re'_k/ϵ was chosen for the necessary role of a weighting factor on x_t.

It remains to determine the quantity ϵ which ideally should be the value of Re'_k at which $x_t = x_k$. This happens to be difficult to determine since x_t may very gradually approach x_k in the limit. Fortunately, the correlations shown later do not seem very sensitive to the value of ϵ except for data in which the Mach number, M_k, is in a certain range around $M_k \approx 1$. The choice of M_k, the local Mach number at the height k in the undisturbed laminar boundary layer at the station x_k, as the parameter most affecting ϵ is based on a study of experimental data. Certainly M_k may not be the only factor—e.g. a Reynolds number or a temperature ratio may be involved—but it appears that M_k is the dominant variable.

Proceeding under the assumption that ϵ is a function of M_k alone, data have been inspected with the aim of establishing this variation. Figure 27 represents the current result. The constant levels of ϵ at low subsonic and high supersonic Mach numbers have been drawn somewhat arbitrarily on the basis of there being

no clear trends away from constant values in those ranges. Data for $0 \leqslant M_k \leqslant 5$ are represented.

The separate curves on figure 27 illustrate an interesting phenomenon, namely the reversal in effectiveness of two- and three-dimensional roughness elements in passing from subsonic to supersonic speed. It should be remembered that Re'_k has been defined the same way for both types of roughness. This may be a factor in the cross over as well as the level of the curves on figure 27, so it is not possible to draw conclusions about the quantitative effectiveness of two- and three-dimensional trips. However, in the present frame of reference a qualitative explanation seems valid. If, as in the present paper, a form of Reynolds number is adopted as the measure of the disturbance due to roughness and yet this number is based on calculated conditions without roughness present, it seems that the two-dimensional element may well appear to produce the greater effective disturbance in subsonic flow where the true velocity and Reynolds number at the top of the element will be greater than for a three-dimensional element. By the same token, the two-dimensional element may suffer greater loss in effectiveness when Mach numbers in the boundary layer become large enough to produce significant shock losses. In that case, true Reynolds numbers at the tops of the elements may not be much different, and the three-dimensional nature of disturbances from that type of element may prevail. One would expect this to occur when M_k becomes somewhat greater than unity. Then, with equal Re'_k the three-dimensional element would appear superior. It must be kept in mind that only three typical types of roughness element are represented in the data analysed in this paper. Thus these comments are not intended to apply to every possible form of roughness element.

The parameters described have been applied to the correlation of typical published data. The position parameter,

$$(x_t/x_{to})^{\frac{1}{2}} - (Re'_k/\epsilon)\,(x_k/x_{to})^{\frac{1}{2}}$$

is plotted as a function of the disturbance parameter Re'_k/ϵ on figure 28. Both two- and three-dimensional roughnesses are included, and Mach numbers from near zero up to five are represented. All data are for bodies having no pressure gradients. The data include cases where k/δ_k ranges from $\frac{1}{10}$ to nearly 4. The bodies represented are flat plates, hollow cylinders, and cones. The values of Re_k required to bring x_t near x_k exceed 20,000 in some of the supersonic flow data.

Boundary-layer trips consisting of a single row of three-dimensional elements obviously admit another variable, namely the lateral spacing of the elements. Earlier experimenters have found that the lateral spacing is not a significant factor within rather wide limits. Klebanoff, Schubauer & Tidstrom (1955) investigated spacings of $\frac{1}{8}$, $\frac{1}{4}$, and $\frac{1}{2}$ in. or 2, 4, and 8 sphere diameters, finding no appreciable effect. Van Driest & McCauley (1958) investigated spacings of $\frac{1}{32}$, $\frac{1}{16}$ $\frac{1}{8}$, and $\frac{3}{16}$ in. without observing an important effect. Spacing of spherical elements was $\frac{1}{8}$ in. for all the VKF tests. With these results in mind, no consideration was given to lateral spacing in the present correlation.

The spherical roughness elements tested by Van Driest & McCauley and by the present researchers were in some cases mounted on thin, two-dimensional bands

which encircled the models. Those used by the former were approximately 0·0012 in. thick and 0·25 in. wide. The VKF tests utilized bands 0·006 in. thick and 0·1875 in. wide. The roughness height, k, in all the following has been taken as the sphere diameter plus the band thickness. In the VKF experiments, k was determined by measuring directly the roughness height on the models.

Values of x_{to} were not determined during the tests reported by Klebanoff *et al.* (1955), so a constant Reynolds number of transition on the smooth plate had to be assumed in order to calculate x_{to} values. There may be some misrepresentation of

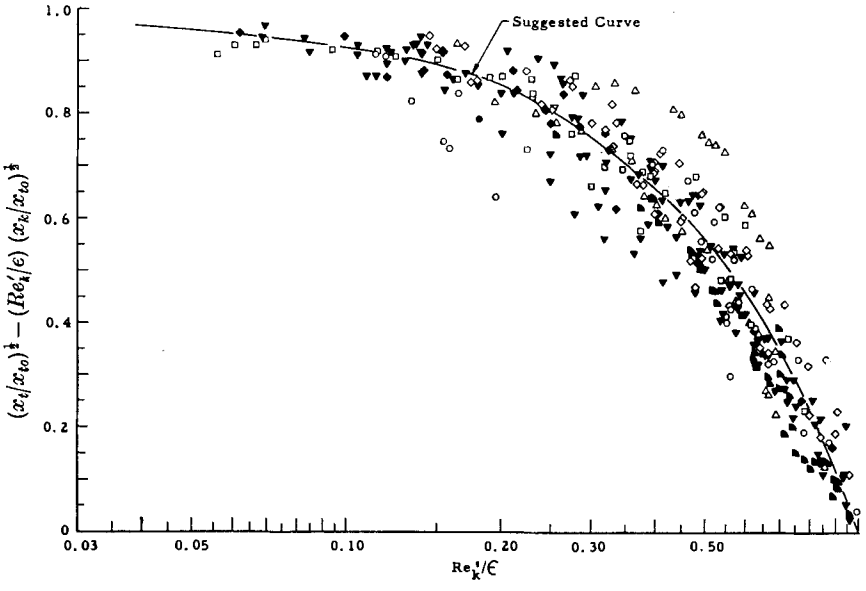

FIGURE 28. Correlation of typical data, $M_\delta \approx 0$ to 5, $T_w \approx T_{aw}$.

Symbol	M_δ	Roughness	Model	Reference
○	1·9–3·7	Row of spheres	Cone	Van Driest & McCauley (1958)
◇	3·0–5·0	Row of spheres	Cylinder	Potter & Whitfield (1960)
□	3·0	Band of grit	Plate	Jones (1959)
▼	3·1	Wire	Cylinder	Brinich (1954)
■	≈0	Wire	Plate	Tani *et al.* (1954)
△	≈0	Row of spheres	Plate	Klebanoff *et al.* (1955)
◆	3·0–5·0	Wire	Cylinder	Potter & Whitfield (1960)

the NBS data in figure 28 because of this, although it is believed small on the basis of a private communication from the experimenters. In this case, then, the use of x_{to} as a reference quantity does not serve to eliminate extraneous effects as it does for the other data.

Only representative experimental data from recent, more extensive tests of bodies without pressure gradients are shown on figure 28. It should be noted that not all data from every source represented in figure 28 have been plotted simply because of the vast quantity of data involved. Selection of data to be shown here has been on a random basis. Data included in figure 28 all apply to bodies with walls at or near adiabatic recovery temperature. Particularly in view of the strong dependence of Re'_k on wall temperature, it is interesting to investigate

situations where Re'_k was varied by changing wall temperature alone (Van Driest & Boison 1957). Figure 29 presents the application of the present procedure to an example of such data. It will be observed that largely satisfactory results are obtained in view of the magnitude of the task attempted.

Since the data in figure 29 also lie reasonably close to the curve established by the data for zero heat transfer, it appears that the single correlation curve in figure 28 may be used for all the cases represented on figures 28 and 29. Closer correlation is exhibited by each of the sets of data when plotted individually. This indicates that reasonably accurate estimates of transition location may be based on this curve. Possession of a means for evaluating the effect of heat transfer on transition due to roughness enables investigation of the transition reversal phenomenon. The experimentally-demonstrated rise and subsequent fall of Re_t with decreasing T_w/T_δ is well known. Some have argued that the increased

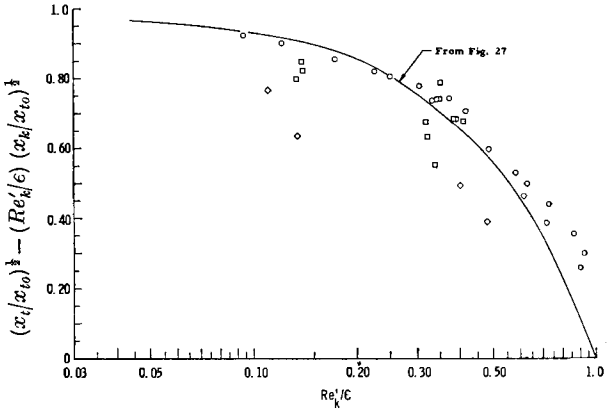

FIGURE 29. Correlation of cold-wall data (single wire on cone). ◇, $M_\delta = 1{\cdot}90$, $(T_w/T_\delta) = 1{\cdot}4$ to $1{\cdot}6$; □, $M_\delta = 2{\cdot}70$, $(T_w/T_\delta) = 1{\cdot}5$ to $2{\cdot}3$; ○, $M_\delta = 3{\cdot}65$, $(T_w/T_\delta) = 1{\cdot}8$ to $3{\cdot}4$ (Van Driest & Boison 1957).

effectiveness of roughness due to wall cooling was not sufficient to explain transition reversal on nominally smooth bodies. However, these discussions have assumed some criterion for transition reversal such as $Re_k > 600$. Using the procedure of the present report leads to an opposite conclusion, as shown by the present authors (1961). The present method for evaluating the effect of roughness will predict reversal on highly cooled bodies with Re_k sometimes much less than 600, particularly when local Mach numbers are low. However, for $T_w = T_{aw}$ and high local Mach numbers, one may find Re_k in the range 10^4 to 10^5.

It is quite likely that the proposed correlation parameters may need modification in order to treat boundary-layer trips of unusual design. For example, it is not obvious that wall temperature is a dominant factor in the case of a hoop raised off the surface, except, of course, through its influence on boundary-layer thickness. In such cases then, one might suspect that wall cooling would be less of a factor in promoting transition due to roughness. An illustration of the trouble encountered in tripping boundary layers on bodies with high local Mach numbers and walls at adiabatic recovery temperature is presented in figure 30. It is clear

that transition in many cases may be accomplished only at the expense of complete disruption of the flow exterior to the boundary layer. Then, the boundary-layer trip, rather than creating circumstances more nearly simulating full-scale free-flight, actually has done the opposite. In cases where bodies with blunt noses and cooled walls are involved, as in hypersonic free flight, there is a strong possibility that the vorticity created by the bow shock wave coupled with the low ratio of T_w/T_0 and low local Mach number may result in far more sensitivity to roughness than indicated by the data discussed here. This must be kept in mind when considering such situations.

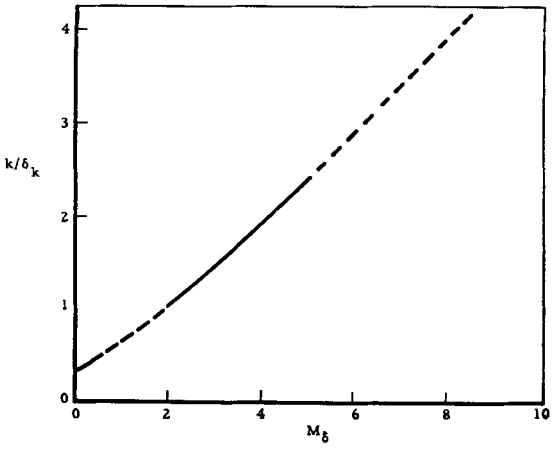

FIGURE 30. Illustration of the increase in roughness size required on adiabatic wall at hypersonic speeds; $x_t = x_k = 2{\cdot}0$ in., $(U/\nu)_\delta = 0{\cdot}3 \times 10^6$/in., $T_w = T_{aw}$; single row of spheres, $Re'_k = 3000$.

8. Concluding remarks

1. Detailed similarity has been noted in the transition process for subsonic, supersonic and hypersonic flows.

2. A marked increase in the magnitude of transition Reynolds numbers has been found in flows at hypersonic Mach numbers. An apparent interrelationship of factors influencing transition does not permit, at present, an isolation of the Mach number influence, per se.

3. The extent of the transition region is shown to increase with increasing transition Reynolds numbers at Mach numbers from zero to eight for flow over adiabatic walls. It increases with Mach number if transition Reynolds number is constant. Quantitative results are given for flow over bodies with no pressure gradients.

4. A critical layer of intense fluctuation-energy concentration in the boundary-layer flow was observed at all Mach numbers studied. This result is in agreement with published results and is to be expected from stability theory. In addition, it is noted that the magnitudes of maximum local fluctuation energies are comparable to those found in fully developed turbulent flow. The distance of this layer from the surface increases with Mach number of adiabatic surfaces.

5. Transition Reynolds numbers are estimated for a vanishingly thin, aerodynamically-flat plate based on an evaluation of leading-edge-geometry effects. Data from several wind tunnels are shown to produce very similar results on this basis. Measured transition Reynolds numbers on cones are shown to be approximately three times the estimated values for aerodynamically-flat plates.

6. Elimination of the influence of leading-edge geometry on flat plates, hollow cylinders, and sharp cones leaves a tendency for increase of transition Reynolds number as unit Reynolds number increases. Factors contributing to this may be present in many experiments, and the possibility should be borne in mind.

7. Parameters which enable a much closer approach to a general correlation of experimental data on boundary-layer transition due to surface roughness are presented. Both two- and three-dimensional roughness in both subsonic and supersonic streams are treated. Correlations of a variety of data are shown for bodies with no pressure gradient, various heat-transfer conditions, and several typical roughness elements. It is remarked that boundary layers on blunt nosed bodies in supersonic flow may exhibit more sensitivity to roughness in some cases. The transition reversal phenomenon whereby Re_t may decrease with T_w/T_δ at very low values of T_w/T_δ appears to be due to surface roughness on the basis of this analysis.

8. Results of the research show that laminar boundary layers on bodies with uncooled, hypersonic boundary layers will be difficult to trip, and the necessary roughness sizes needed will frequently create serious flow distortions extending well outside the boundary layer. In the case of large Mach numbers, the required size of roughness is shown to increase approximately exponentially with M_δ on bodies with no pressure gradient when wall temperature equals adiabatic recovery temperature and unit Reynolds numbers are equal. A cooled wall required less roughness for otherwise equal conditions.

This research was supported by the United States Air Force, Air Research and Development Command, under Contract Number AF 40(600)-800, Program Area 750A, Proj. no. 8953.

The authors are indebted to J. C. Donaldson, Max Kinslow, W. M. Crouch, and R. D. Fisher, Jr., who made significant contributions in the experimental phases of this project, and to Mrs Betty M. Majors who performed most of the calculations.

REFERENCES

Anderson, A. 1958 *AEDC-TN-58-8.*

Battin, R. H. & Lin, C. C. 1950 *J. Aero. Sci.* **17**, 453.

Bennett, H. W. 1953 *Kimberly-Clark Corporation*, Neenak, Wisconsin, private report.

Bertram, M. H. 1957 *NACA Rep.* no. 1313.

Braslow, A. L. & Knox, E. C. 1958 *NACA TN* no. 4363.

Brinich, P. F. 1954 *NACA TN* no. 3267.

Brinich, P. F. & Sands, N. 1957 *NACA TN* no. 3979.

Chapman, D. R., Kuehn, D. M. & Larson, H. K. 1957 *NACA TN* no. 3869.

Coles, D. 1953 *Jet Propulsion Laboratory Rep.* no. 20-71.

Demetriades, A. 1958 *California Institute of Technology GALCIT Memorandum* no. 43.

DRYDEN, H. L. 1953 *J. Aero. Sci.* **20**, 477.

FAGE, A. 1943. *Aero. Res. Coun., Lond., R & M* no. 2120.

FEINDT, E. G. 1956 *Jahrbuch der Schiffbautechnischen Gesellschaft*, **50**.

GIBBINGS, J. C. 1958 *Aero. Res. Coun., Lond., FM* 2754.

JONES, R. A. 1959 *NASA Mem.* no. 2–9–59L.

KLEBANOFF, P. S., SCHUBAUER, G. B. & TIDSTROM, K. D. 1955 *J. Aero. Sci.* **22**, 803.

KLEBANOFF, P. S. & TIDSTROM, K. D. 1959 *NASA TN* no. D-195.

KOVASZNAY, L. S. G. 1954 *NACA Rep.* no. 1209.

LAUFER, J. & MARTE, J. E. 1955 *Jet Propulsion Laboratory Rep.* no. 20–96.

LAUFER, J. & VREBALOVICH, T. 1958 *Jet Propulsion Laboratory Report* no. 20-116.

LAUFER, JOHN 1961 *J. Aero. Sci.* **28**, 685.

POTTER, J. L. 1957 *J. Aero. Sci.* **24**, 158.

POTTER, J. L. & WHITFIELD, J. D. 1960 *AGARD Boundary Layer Research Meeting, London.* (AEDC-TR-60-5).

POTTER, J. L. & WHITFIELD, J. D. 1961 *J. Aero. Sci.* **28**, 663.

RAYLEIGH, LORD *Proc. Lond. Math. Soc.* **11**, 57 (1880) and **19**, 67 (1887); (*Scientific Papers*, I, 474 and III, 17); see also *Scientific Papers*, IV, 203 (1895) and VI, 197 (1913).

RUMSEY, C. B. & LEE, D. B. 1956 *NACA RM* L56 B07.

RUMSEY, C. B. & LEE, D. B. 1958 *NACA RM* L57 J10.

SCHILLER, L. 1932 *Handbuch der Experimentalphysik*, Vol. 4, Part 4, pp. 189–192. Leipzig.

SCHLICHTING, H. 1955 *Boundary-Layer Theory.* New York: McGraw-Hill Book Company.

SCHUBAUER, G. B. & SKRAMSTAD, H. K. 1948 *NACA Rep.* no. 909.

SILVERSTEIN, ABE & BECKER, JOHN V. 1938 *NACA Rep.* no. 637.

SIVELLS, JAMES C. 1959 Paper presented at joint meeting of the STA–AGARD Wind Tunnel and Model-Testing Panel, Marseilles, France, September 1959.

SMITH, A. M. O. & CLUTTER, D. W. 1957 *Douglas Aircraft Company, Rep.* no. ES 26803.

SMITH, A. M. O. & CLUTTER, D. W. 1959 *J. Aero. Sci.* **26**, 229.

SMITH, A. M. O. & CLUTTER, D. W. 1960 *J. Aero. Sci.* **27**, 70.

TANI, I., HAMA, F. R. & MITUISI, S. 1954 *Rep. Inst. Sci. Tech., Univ. Tokyo*, **8**, no. 3.

VAN DRIEST, E. R. & BOISON, J. C. 1957 *J. Aero. Sci.* **24**, 885.

VAN DRIEST, E. R. & MCCAULEY, W. D. 1958 *North American Aviation, Inc., Aero-Space Lab. AFOSR TN*-58-176.

WHITFIELD, J. D. & POTTER, J. L. 1958 *AEDC-TN*-58-77.

WINTER, K. G., SCOTT-WILSON, J. B. & DAVIES, F. V. 1954 *Roy. Aircraft Est. TN Aero* no. 2341.